2012

Base-caged Adenosine Triphosphate as a Model System for Photoactivatable Small Interfering RNA

Amanda Yoesting Hendrix
Louisiana State University and Agricultural and Mechanical College

BASE-CAGED ADENOSINE TRIPHOSPHATE AS A MODEL SYSTEM FOR PHOTOACTIVATABLE SMALL INTERFERING RNA

A Thesis

Submitted to the Graduate Faculty of the
Louisiana State University and
Agricultural and Mechanical College
In partial fulfillment of the
Requirements for the degree of
Master of Science in Biological and Agricultural Engineering

in

The Department of Biological and Agricultural Engineering

Amanda Y. Hendrix
B.S., Oklahoma State University, 2005

August 2012

ACKNOWLEDGEMENTS

First and foremost, I thank Dr. W. Todd Monroe for recruiting me to the Biological & Agricultural Engineering Department, both as a Teaching Associate and a graduate student. None of this would have been possible without his guidance and encouragement. I also thank my committee members Drs. Daniel Hayes and Evgueni Nesterov for their expertise, time, and invaluable support.

This multi-faceted project required assistance from several different areas. A huge thank you to the following folks who helped with different portions of the project: Drs. Ted Gauthier and Tamara Chouljenko for their help in running the luminometer, and Dr. Connie David for her work with mass spectrometry. In Dr. Nesterov's lab, several people were great resources in assisting with the NMR component of my research: Dr. Jinwoo Choi, Rajib Mondal, and Deepa Pangeni.

In the BAE department, I owe a huge thank you to BAE administrative staff: Mrs. Angela Singleton, Mrs. Rhonda Shepard, and Mrs. Donna Elisar. I also thank Alyson Moll and Ammar Qureshi for their assistance in the lab. Last but not least, a very special thanks to Laura DeLatin for her dedication and assistance in working with me on this project.

Finally, I thank my family for their love and support as I have worked on this new path in my life: my husband Jake Hendrix and my parents Kent and Cindy Yoesting.

TABLE OF CONTENTS

LIST OF TABLES

LIST OF FIGURES

ABSTRACT

Photocaged adenosine triphosphate (ATP) is one of the earliest examples of exerting spatial-temporal control over the activity of a substrate. The activity of ATP is blocked until near-ultraviolet light exposure photocleaves the cage moiety. Caged ATP has been used for a myriad of applications including kinetic studies of ATP-dependent enzymes. Traditional caging of ATP occurs at the γ-phosphate, which has been found to competitively inhibit several enzymatic systems. It was hypothesized that blocking access to the adenosine N^6 position via cage molecule would prevent the initial enzyme-substrate binding event from occurring prior to photolysis, effectively minimizing competitive inhibition. Utilizing a convertible nucleoside analog of ATP, this work synthesized, purified, and characterized a form of caged ATP which, by attaching the cage molecule to the nucleobase, did not inhibit the enzymatic activity of luciferase *in vitro*. Characterization was accomplished via UV/Vis spectroscopy, high performance liquid chromatography (HPLC), nuclear magnetic resonance (NMR), and mass spectrometry (MS). Base-caged ATP was evaluated in a firefly luciferase enzymatic assay to determine the degree of bioactivity in the caged and photoactivated states and compared to the results of native (uncaged) ATP and γ-NPE-caged ATP. Photolysis was conducted via 308 nm light from a transilluminator. Base-caged ATP did not inhibit the enzymatic system and the convertible nucleoside synthesis approach offers significant advantages over other caging techniques.

CHAPTER 1 – BACKGROUND AND SIGNIFICANCE

1.1 Objectives

Base-caged adenosine triphosphate as a model system for photoactivatable siRNA.

1. Synthesize base-caged ATP.
2. Purify base-caged ATP through separation techniques.
3. Characterize results through analytical chemistry.
4. Demonstrate:
    A. Bio-inactive in base-caged form;
    B. Photolysis restores bioactivity;
    C. Confirm that base-caged form does not inhibit enzymatic systems.

1.2 Introduction

Developments in the field of tissue regeneration and engineering include advances in the use of biomaterials and stem cells, scaffolds, growth and differentiation factors, and biomimetic environments to achieve three-dimensional cell cultures (Takahashi, Ogasawara et al. 2007). Despite numerous improvements, much work remains to perfect clinically applicable growth of complex tissues. One of the primary challenges in tissue growth arises from the lack of complex control techniques to direct pluripotent cell differentiation.

A plausible method to enhance tissue repair and regeneration is by the modification and exploitation of the RNA interference (RNAi) mechanism to silence gene expression (Mack 2007; Casey, Blidner et al. 2009). Spatial-temporal control is introduced when RNAi techniques are coupled with an external trigger through the utilization of photocaging. Photocaging involves chemically modifying the molecule of interest with a photolabile compound that inhibits

bioactivity until released with a specific wavelength of light (Casey, Blidner et al. 2009). As such, caged RNA oligonucleotides are inactive and do not participate in RNAi until exposed to light, which can be readily pinpointed with temporal and spatial precision.

The primary aim of this work was to develop a precise photocaging process utilizing base-caged adenosine triphosphate (ATP) as a model system for the RNA nucleoside adenosine.

1.3 RNA Interference

The first element of directed tissue growth and regeneration stems from the discovery of RNA interference (RNAi). RNAi plays a large role in determining the activity of genes by turning them on, off, up regulating, or down regulating their expression. The manipulation of gene expression with RNA was revolutionized by the findings of Nobel laureates Fire and Mello, who were among the first to characterize and exploit RNAi through the use of small double-stranded RNA molecules known as small interfering RNAs (siRNAs) (Fire, Xu et al. 1998). Subsequent studies have shown that cell differentiation and proliferation can be regulated via RNAi gene silencing (Chen, Mandel et al. 2006). Transient inhibition with siRNAs would enable the finely tuned regulation of cell differentiation that is needed for the successful growth of musculoskeletal tissue *in vitro* (Rhim, Lowell et al. 2007).

1.3.1 RNA Interference Mechanism

RNA interference is a post-transcriptional gene regulation mechanism in eukaryotic organisms. The aforementioned small interfering RNAs (siRNAs) comprise a class of dsRNA of 20-25 nucleotides in length. Native RNAs which participate in this pathway are single-stranded

RNA called microRNAs (miRNAs) of 21-25 nucleotides in length (He and Hannon 2004). The expression of a specific gene is moderated by miRNAs or siRNAs which hybridize with a complementary strand of mRNA. This hybridization silences the mRNA's activity by repressing translation or cleaving the mRNA (He and Hannon 2004; Gregory, Chendrimada et al. 2005; Rhim, Lowell et al. 2007).

Native miRNA genes contain one or more 60-120 nucleotide-long segments exhibiting sufficient reverse sequence complementarity to spontaneously form hairpin-loop structures (Hartwell, Hood et al. 2008). The initial transcription product is known as primary miRNA (pri-miRNA). After transcription, the pri-miRNA is recognized by the nuclear enzyme *Drosha*, which crops the RNA at the base of the structure to remove the 5' mG cap and the 3' poly-A tail (Hartwell, Hood et al. 2008). *Drosha* releases a 65-75-nt form called pre-miRNA which is transported to the cytoplasm by Exportin-5-mediated nuclear transport (Yi, Qin et al. 2003). Once in the cytoplasm of the cell, a ribonuclease (RNase-III) called *Dicer* recognizes the pre-miRNA. *Dicer* cuts the loop off the pre-miRNA to produce the mature 21-24 ribonucleotide miRNA and its complement miRNA* (He and Hannon 2004; Hartwell, Hood et al. 2008). When long dsRNA molecules are found in the cytoplasm, *Dicer* also processes these into siRNA duplexes (He and Hannon 2004). These duplexes are further processed by a ribonucleoprotein effector complex called the RNA-induced silencing complex (RISC) (Gregory, Chendrimada et al. 2005). The RNase component of the RISC degrades the miRNA* and complementary siRNA strands (He and Hannon 2004; Winter, Jung et al. 2009), and the miRNA/siRNA-loaded RISC complex (miRISC/siRISC) becomes an active agent of RNA interference. The formation of miRNA and siRNA silencing complexes are graphically shown in **Figure 1**.

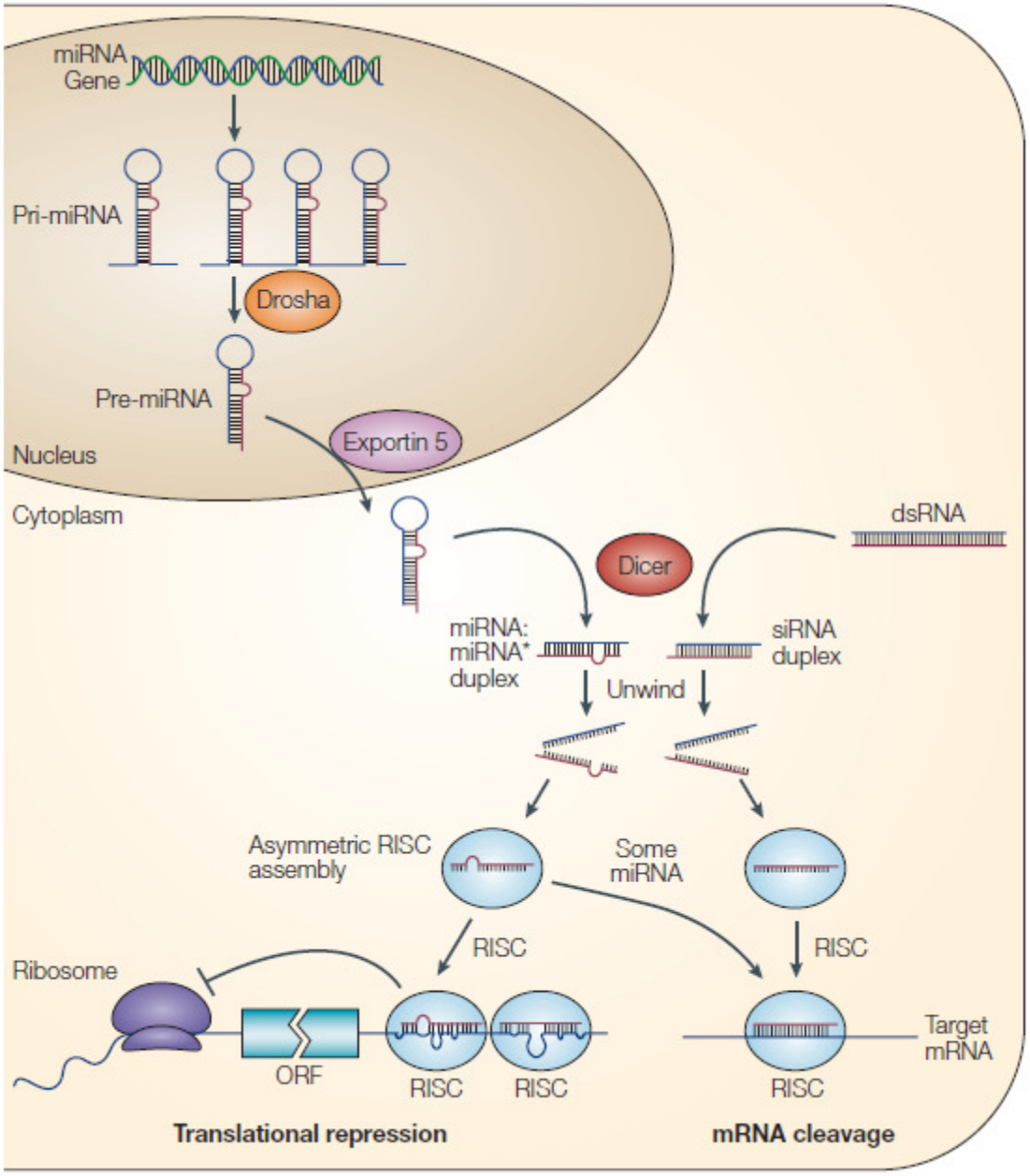

Figure 1 – Model for the biogenesis and post-transcriptional suppression by miRNAs and siRNAs.

Initial primary microRNA (pri-miRNA) transcripts are cleaved inside the nucleus into 65-75-nt pre-miRNAs by *Drosha*. Pre-miRNAs are transported to the cytoplasm by Exportin 5 and are processed into miRNA:miRNA* duplexes by *Dicer*. *Dicer* also cleaves long dsRNA molecules into siRNA duplexes. Only one strand of the miRNA:miRNA* duplex or the siRNA duplex is assembled into the RNA-induced silencing complex (RISC). The assembled RISC translationally represses or cleaves mRNAs depending on the degree of complementarity between the miRNA or siRNA and the target mRNA. Reprinted by permission from Macmillan Publishers Ltd: *Nature Reviews Genetics* **5**, 522-531 (July 2004), copyright 2004.

RNA interference exhibits two forms of post-transcriptional control of gene expression, as seen in **Figure 1**. The precise mode of RNAi depends on the degree of complementarity between the miRNA or siRNA and the target mRNA (He and Hannon 2004; Hartwell, Hood et al. 2008). The first mode occurs when the miRISC/siRISC sequence hybridizes in a perfectly base-paired complex with the mRNA; the miRISC/siRISC then cleaves the mRNA (Esquela-Kerscher and Slack 2006). Because the products of cleavage are not protected by a 5' mG cap or 3' poly-A tail, they degrade in the cytoplasm. The miRISC/siRISCs are therefore recyclable catalysts and continue to bind to additional mRNA targets. Small amounts of miRNA/siRNA can have a dramatic effect in down-regulating or silencing gene expression (Hartwell, Hood et al. 2008).

A translational blockage occurs when the miRISC/siRISC sequence forms an imperfect hybrid with the mRNA. In this case, the mRNA remains intact and loads into ribosomes. However, the miRISC/siRISC represses the movement of the ribosomes, leading to the down-regulation of translation (Hartwell, Hood et al. 2008).

1.3.2 RNAi-promoted Cell Proliferation and Differentiation

The involvement of miRNAs in the proliferation and differentiation of skeletal muscle was demonstrated by Chen et al. Their findings presented evidence that the studied miRNAs acted as post-transcriptional repressors that controlled myogenesis, or the formation of skeletal muscle tissue (Chen, Mandel et al. 2006). Specifically, miR-1 was found to induce the expression of myogenic markers in cells that were proliferated in the log-phase of growth. These markers resulted in accelerated myogenic differentiation. Another miRNA, miR-133, was found to promote myoblast proliferation. The interplay between the proliferation and differentiation of

myoblasts, the precursors of skeletal muscle, plays a key role in the regenerative growth of skeletal muscle tissue.

With the establishment of the involvement of miRNAs in muscle tissue growth, Rhim *et al.* found that the *transient* inhibition of miRNAs would enable the finely tuned regulation of cell differentiation that is needed for the successful growth of musculoskeletal tissue *in vitro* (Rhim, Lowell et al. 2007). The approach to developing a control strategy for directed cell differentiation is therefore focused on delivering siRNAs to silence either mRNA or miRNA at varying times and spatial locations.

A couple strategies to accomplish spatial and temporal control of RNA molecules have been employed in recent work, primarily based on the use of external triggers. One method exerts remote electronic control over the hybridization of DNA molecules through inductive coupling a radio-frequency magnetic field to a metal nanocrystal antenna covalently linked to a DNA oligonucleotide (Hamad-Schifferli, Schwartz et al. 2002). The external trigger technique investigated in this work utilizes chromophores to optically trigger biomolecular activity in a field known as photocage chemistry.

1.4 Photochemistry and Cage Compounds

1.4.1 Caging via Photochemistry

In addition to the need for transient gene silencing for optimal proliferation and differentiation of myoblasts, flooding an organism with active siRNAs would be unsafe. The downstream effects of widespread gene silencing that could occur in off-target tissues would have unpredictable results. The chosen approach to achieve spatiotemporal control of siRNA

molecules is to utilize a photolabile protecting group known as a "cage" (Givens, Kotala et al. 2005).

Caging specifically describes the attachment of a photolytic chromophore for the prompt release of a biologically active substrate (Kaplan, Forbush et al. 1978). By covalently alkylating an isolated nucleic acid with a photolabile cage, the bioactivity of the nucleic acid is blocked. Upon exposure to the appropriate wavelength of light (**Figure 2**), the caging group photocleaves and restores the nucleic acid to its original bioactive state (Casey, Blidner et al. 2009), thus enabling a system of control over the location and timing of the siRNA activity. Finer control is achieved by varying the location, intensity, and duration of the light pulse delivered to uncage the molecule of interest (Givens, Kotala et al. 2005). No further photoactivation occurs in the absence of light, so the delivery of light in a step function technique will allow for the controlled activation of nucleic acids, only activating a portion of the siRNAs at a time (Casey, Blidner et al. 2009).

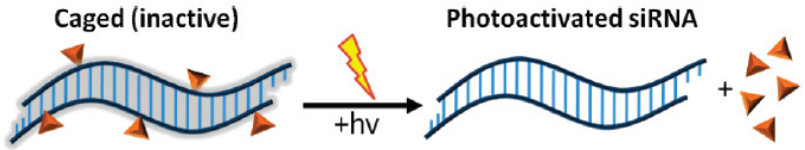

Figure 2 – Caged siRNA
Caged siRNA is biologically inactive until UV light exposure cleaves the cage moieties, enabling initiation of gene silencing (Casey, Blidner et al. 2009).

Photocaging offers advantages for the delivery of siRNAs by allowing the dispersal of the biologically inert siRNAs with minimized risk of initiating gene silencing in off-target tissues. Caged siRNAs could conceivably be introduced intravenously for activation in a specific location of interest. Therefore, the photocaged siRNAs offer a major advantage over conventional delivery methods of gene silencing (Givens, Weber et al. 1998). However, the

photocaging process is not always perfect; small amounts of "leak," or bioactivity in the non-photolyzed state, could lead to gene silencing in unintended tissues and have an effect on study results (Casey, Blidner et al. 2009).

Caged nucleic acids were first demonstrated *in vitro* and *in vivo* for photoinduced control of gene expression in 1999 (Monroe, McQuain et al. 1999). Two classifications of caged nucleic acid molecules have emerged: those that were caged using a random method termed "statistical caging" (Mayer and Heckel 2006), and more recent site specific approaches to photocage predetermined sites on knockdown oligonucleotides (Casey, Blidner et al. 2009). Statistical caging, also known as bulk caging, uses a batch-style reaction to attach the cage molecule to the phosphate backbone using diazo attachment chemistry (Walker, Reid et al. 1988; Monroe, McQuain et al. 1999; Casey, Blidner et al. 2009). Limitations of this method include significant leak activity (Shah, Rangarajan et al. 2005) and evidence of a 2′-hydroxyl attack at the phosphotriester backbone (Breslow and Xu 1993). Further in-depth review of caged nucleic acids is offered by Casey *et al.* (Casey, Blidner et al. 2009).

1.4.2 Cage Compounds

A variety of cage compounds have been studied since 2-nitrobenzyl was used to cage ATP (Kaplan, Forbush et al. 1978). Success as a cage compound requires ease of synthesis of the effector-cage complex and efficiency of photochemical release of the effector (Givens, Kotala et al. 2005). Based on these criteria, only four categories of cage compounds are currently considered robust enough for use: (1) 2-nitrobenzyl (2-NB), (2) benzoin, (3) *p*-hydroxyphenacyl, and (4) arylmethyl derivatives including the benzyl and coumaryl

chromophores (Givens, Kotala et al. 2005). The chemical structures of several photocaging groups are shown in **Figure 3**.

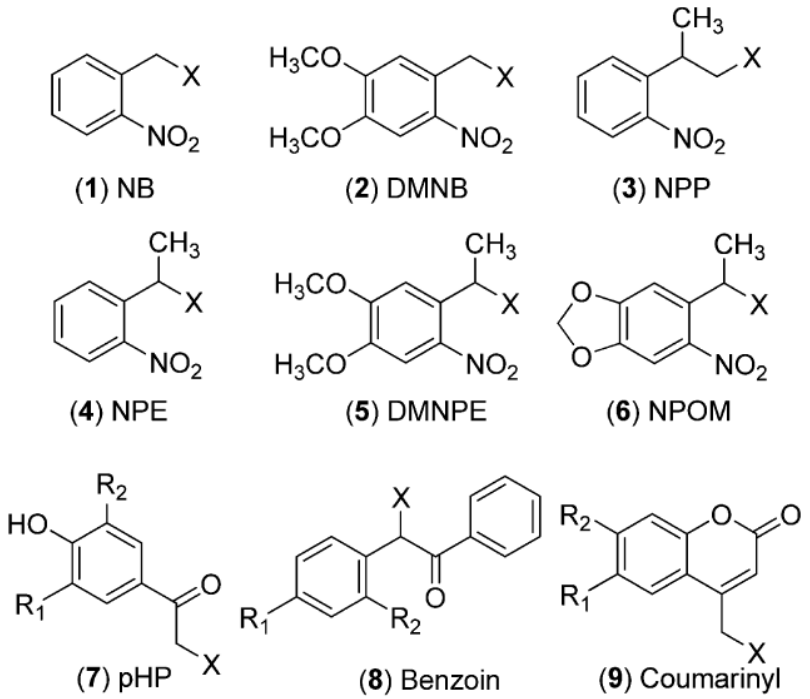

Figure 3 – Common cage compounds for use with siRNAs
X = substrate, NB = nitrobenzyl, DMNB = dimethoxy-nitrobenzyl, NPP = nitrophenylpropyl, NPE = nitrophenylethyl, DMNPE = dimethoxy-nitrophenylethyl, NPOM = 6-nitropiperonyloxymethyl, *p*HP = *p*-hydroxyphenacyl (Casey, Blidner et al. 2009).

The best characterized and most widely utilized cage molecules come from the 2-nitrobenzyl group and its derivatives (Casey, Blidner et al. 2009). More in-depth reviews of cage compounds are offered by Givens and Casey (Givens, Kotala et al. 2005; Casey, Blidner et al. 2009).

For this work, 2-nitrobenzyl was selected due to its robust properties as a cage molecule and its ease of attachment in synthesis reactions. In addition, 2-nitrobenzyl groups exhibit

reliably high photorelease efficiencies due to the irreversible photoredox mechanism shown in **Figure 4** (Givens, Kotala et al. 2005).

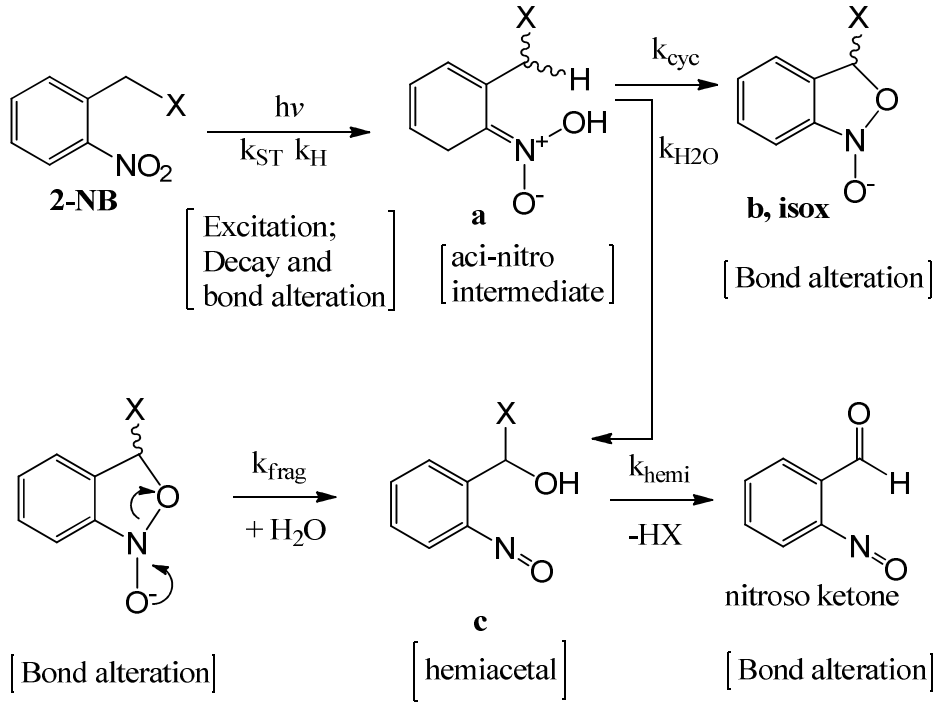

Figure 4 – General mechanism for 2-nitrobenzyl photorelease of a substrate.
X = substrate. Rate constants are: k_{ST} = single-triplet crossing; k_H = hydrogen abstraction; k_{cyc} = cyclization to the isoxazole; k_{H2O} = direct hydrolysis to the isoxazole; k_{frag} = fragmentation of the isoxazole; k_{hemi} = hemiacetal or ketal hydrolysis. Intermediate states are labeled **a**, **b**, and **c**. Adapted from (Givens, Kotala et al. 2005).

1.4.3 Convertible Nucleoside Approach

One method to obtain photolabile protecting groups on the nucleobase is the post-synthesis substitution of the oligonucleotide. A group led by Verdine developed a method for incorporating reactive nucleotide analogs with protecting groups stable under the conditions of RNA solid-phase synthesis, but able to undergo substitution for post-synthetic placement of the cage compound. They named their technique "the convertible nucleoside approach" (Ferentz and Verdine 1992; Ferentz, Keating et al. 1993). This method offers an advantage over the site-

specific modified phosphoramidite approach in which the 2′-hydroxyl of RNA is caged (Chaulk and MacMillan 2007). Although the caged adenosine phosphoramidite is easily incorporated into short oligonucleotides by automated synthesis, the protected adenosine requires an extensive synthesis procedure (Chaulk and MacMillan 2007; Casey, Blidner et al. 2009). In contrast, the photoprotecting synthesis through the convertible nucleoside approach is much simpler and requires fewer reagents. The cage compound conversion reaction requires a primary amine that is nucleophilic in order to undergo nucleophilic aromatic substitution, shown in **Figure 5** (Allerson, Chen et al. 1997).

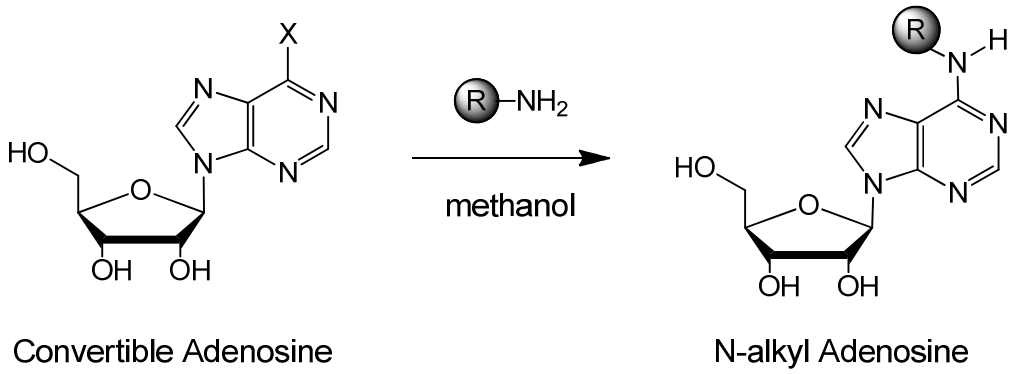

Figure 5 – Amine Substitution of Adenosine Nucleoside
Generalization of the reaction to alkylate convertible adenosine nucleosides using aminolysis or nucleophilic aromatic substitution. X = leaving group, R = cage group. (Allerson, Chen et al. 1997).

Using this convertible nucleoside method, Verdine's group successfully demonstrated the conversion of a modified adenosine molecule using benzylamine, shown in **Figure 6** (Allerson, Chen et al. 1997). This generated a modification which attached benzylamine to the N^6 position of adenosine. From this synthesis reaction, Blinder developed a similar synthesis procedure to attach the 2-nitrobenzylamine (NB-NH_2) cage molecule to the N^6 position of adenosine, discussed in Section 2.3.1.

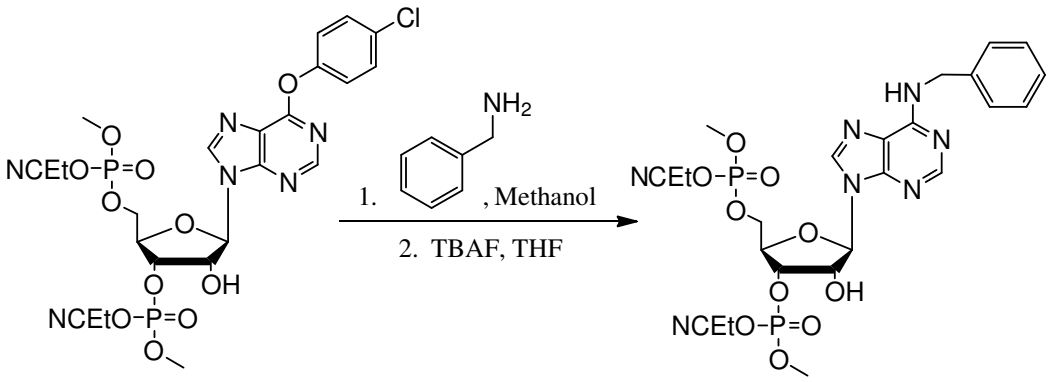

Figure 6 – Convertible Adenosine Reaction

The future implications of this work, together with the convertible nucleoside approach, will allow for the site-specific photocaging of RNA oligonucleotides. RNA oligos can be

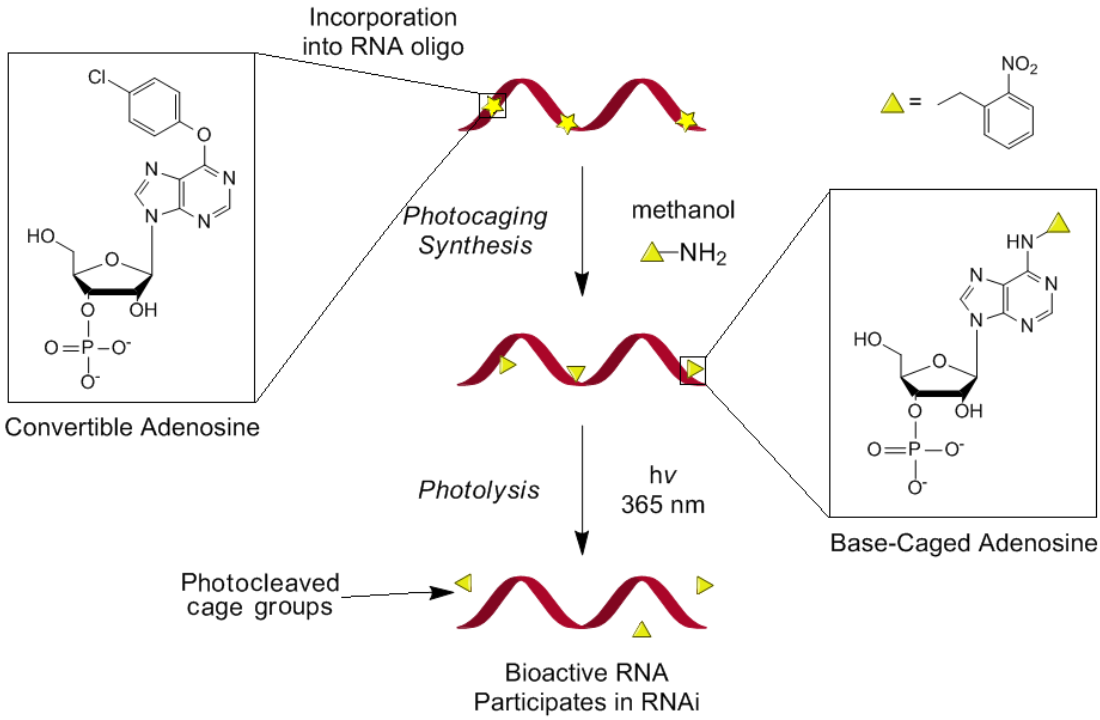

Figure 7 – Convertible adenosine incorporation into RNA oligo

manufactured with a DNA/RNA synthesizer, and the identified adenosine nucleosides can be substituted for a convertible nucleoside. Synthesis techniques would then be applied to the oligo to modify the convertible nucleoside into a photocaged adenosine (**Figure 7**).

1.5 ATP as a Model System for RNA

Adenosine triphosphate (ATP) is widely recognized for its central role in intracellular energy transfer due to its involvement in cellular control mechanisms and metabolic processes (Knowles 1980). Caged ATP provides an excellent model for testing caging synthesis protocols. Historically, caged ATP was one of the first examples of the application of photochemistry to exert control over the biological activity of a substrate (Kaplan, Forbush et al. 1978; Blidner 2007). In the first study by Kaplan, 2-nitrobenzyl and 1-(2-nitrophenyl)ethyl groups were attached to the gamma phosphate of ATP to control the activity of a Na:K ATPase ion pump (Kaplan, Forbush et al. 1978). Since then, caged ATP has been used for a myriad of applications, especially for kinetic studies of ATP-dependent enzymatic studies including the Na,K-ATPase pump (Kaplan, Forbush et al. 1978; Forbush 1984; Geibel, Barth et al. 2000), transport by the mitochondrial ADP/ATP carrier (AAC) (Broustovetsky, Bamberg et al. 1997; Gropp, Brustovetsky et al. 1999), kinesin (Higuchi, Muto et al. 1997), and myosin/actomyosin (Thirlwell, Corrie et al. 1994). Many of these applications utilize the nitrobenzyl cage group with γNPE caged ATP (Kaplan, Forbush et al. 1978; Forbush 1984; Broustovetsky, Bamberg et al. 1997; Higuchi, Muto et al. 1997; Gropp, Brustovetsky et al. 1999). Other studies have used other cage molecules, such as DMB-caged ATP (Thirlwell, Corrie et al. 1994) and pHP-caged ATP (Geibel, Barth et al. 2000).

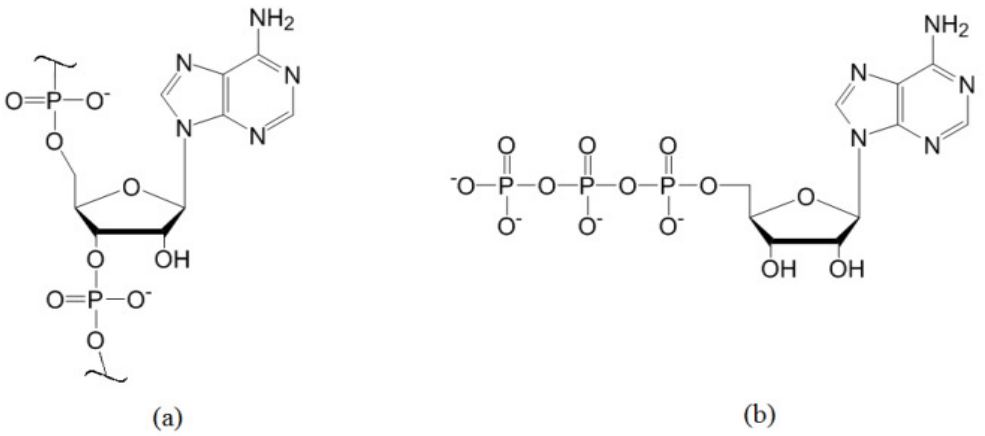

Figure 8 – Structures of (a) chain-form adenosine in RNA, (b) adenosine-5'-triphosphate

In addition to the ubiquitous application of ATP in enzymatic assays, ATP can be used as a model for the adenosine nucleotide in RNA due to the inherent similarity of structure, shown in **Figure 8**. This structural similarity will allow similar synthesis techniques to be conducted on ATP analogs and adenosine convertible nucleosides.

1.5.1 Gamma-Phosphate Caged ATP

Traditional caging of ATP has been achieved via the alkylation of the gamma phosphate. Although the γ-phosphate caged ATP does inhibit kinase activity, protein-ATP binding has been reported to occur regardless of the cage status. This interference of caged ATP in an enzymatic system was first identified by Forbush with the discovery that ATP, caged at the γ-phosphate, binds to Na^+:K^+-ATPase with a greater affinity than uncaged ATP (Forbush 1984). This caused unphotolyzed caged ATP to occupy the catalytic sites of the Na^+ pumps prior to the photolysis flash. Forbush found that most of the free ATP is produced in solution while only about 2% of the bound caged ATP converted to ATP (Forbush 1984). Consequently, ATP caged at the γ-phosphate competitively inhibits the Na^+:K^+-ATPase pump.

The competitive inhibition of ATP binding by NPE γ-phosphate caged ATP was further observed in other enzymatic systems. Thirlwell et al. found evidence indicative of inhibition in the relaxation of muscle fibers with actomyosin ATPase (Thirlwell, Corrie et al. 1994). Caged ATP was also found to inhibit ATP-driven sliding of kinesin and microtubules in motility assays (Higuchi, Muto et al. 1997). Competition between caged and free ATP in mitochondrial ADP/ATP carrier protein studies indicated that the caged form had stronger affinity with the protein binding site than native ATP (Broustovetsky, Bamberg et al. 1997). The competitive inhibition is not limited to the 2-NB and NPE cage molecules in the γ-phosphate caged ATP; the Na^+:K^+-ATPase also undergoes competition with *p*-hydroxyphenacyl (pHP)-caged ATP (Geibel, Barth et al. 2000). Since many of these enzymatic systems are specific to adenosine triphosphate, this work strives to cage the adenine nucleobase in order to determine if competitive inhibition is lessened, while still blocking the bioactivity of ATP. Caging the adenine nucleobase at the N^6 position, using the convertible alkylation schemes discussed in Section 1.3.3, may provide spatial-temporal control over the biological activity of ATP without engaging in the competitive inhibition of free ATP. Although recent work has resulted in advances in nucleobase caging of oligonucleotides (Hobartner and Silverman 2005), synthesis of base-caged ATP had not been investigated until recently (Blidner 2007).

1.5.2 Enzymatic Binding of ATP and Base-Caged ATP Hypothesis

For this work, a luciferin/luciferase ATP reporter assay was selected as the *in vitro* system for studying caged ATP due to its well-characterized linear response and inherent hydrolysis of ATP. Additionally, luminescence produced by the assay allows for the quantification of native ATP, caged ATP, and photolyzed ATP species.

Support for caging the N^6 position of ATP comes from literature describing the molecular binding of ATP to proteins and enzymes. For example, firefly luciferase has a long history of biochemistry and kinetic studies, including the determination of the ATP binding site. As long ago as 1970, Lee, Denburg, and McElroy found the 6-amino group of adenine to be critical for the adenylate intermediate binding required to produce the luciferase luminescence (Lee, Denburg et al. 1970). They also found that the energetic contributions to ATP-luciferase binding come from the adenine ring and the α phosphate group. These findings implicate the N^6 ATP group as a key player in ATP-luciferase binding.

Twenty-six years later, firefly luciferase was the first enzyme of its class to be crystallographically characterized, further elucidating the structures of the adenylate-forming enzyme superfamily (Conti, Franks et al. 1996). The crystal structure supported the theory that luciferase correctly positions and stabilizes binding of ATP for catalyzing adenylate formation, beginning the cascade to produce luminescence. A more recent study used the Protein Data Bank to mine for molecular recognition of the adenine moiety of ATP by proteins (Mao, Wang et al. 2004). They found that nearly 59% of adenylate-protein complexes involve the N^1 and N^6 atoms of the adenine base via the formation of dual hydrogen bonds, and hydrogen bond formation was even higher (85%) for the N^6 position overall.

Based on the review of ATP binding in literature, we hypothesize that blocking access to the 6-amino group via cage molecule will prevent the initial enzyme-substrate binding event from occurring prior to photolysis, effectively minimizing competitive inhibition. This hypothesis is depicted schematically in **Figure 9**.

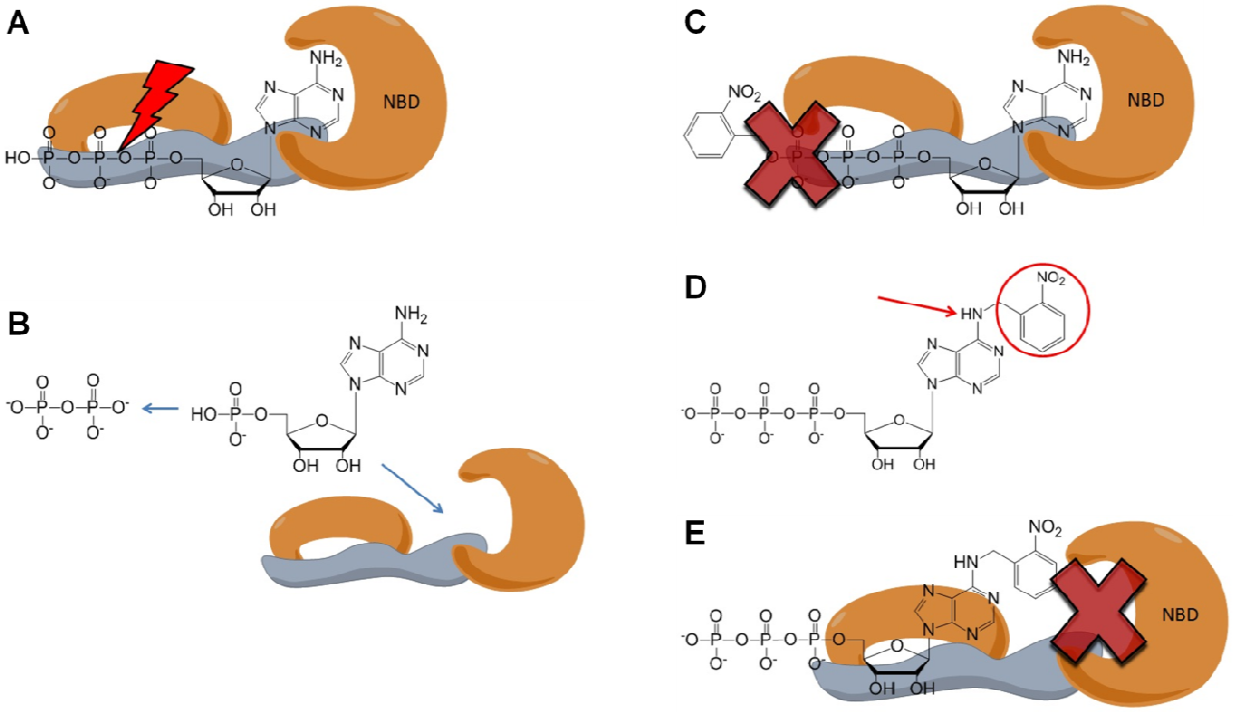

Figure 9 – N^6 caged ATP (BC-ATP) Hypothesis
A. Schematic representation of ATP hydrolysis by luciferin/luciferase: the enzyme nucleotide binding domain (NBD) binds ATP at the adenosine. B. Following hydrolysis, the enzyme releases AMP and pyrophosphate. C. Enzyme binds γNPE-ATP at the adenosine, but hydrolysis is blocked by the cage molecule. D. Location of cage molecule attachment on proposed base-caged ATP. E. Hypothesis: attachment of cage molecule to N^6 of adenosine prevents binding to NBD of enzyme, therefore preventing competitive inhibition.

The ATP binding site of the enzyme is designated here as the nucleotide binding domain (NBD), but it is alternatively referred to as the adenylate binding site.

CHAPTER 2 – EXPERIMENTAL DESIGN

2.1 Previous Work

Investigation of base-caged ATP was previously conducted by Rick Blidner as part of his dissertation research in the Biological & Agricultural Engineering Department at Louisiana State University (Blidner 2007). The continuance of his work is prompted by the promising results indicated by a luciferase ATP assay (**Table 1**), in which enzyme activity (measured as luminescence) was documented prior to and following photoexposure using ATP, 1-(2-nitrophenyl)ethyl (NPE) γ-phosphate caged ATP, and 2-nitrobenzylamine (NB-NH_2) base-caged ATP (Blidner unpublished data). The base-caged ATP products were synthesized using the modified nucleoside technique mentioned in Section 1.4.3. Both caged ATP analogues demonstrated photoactivation, and NB-NH_2 base-caged ATP exhibited greater caging efficacy than NPE γ-phosphate-caged ATP as seen by the incomplete suppression of bioactivity while caged, or leak activity, of γ-phosphate NPE caged ATP. The crude base-caged ATP products could be tested without purification because the unreacted 6-chloropurine riboside triphosphate (CPR-TP) has negligible activity in the luciferase reporter assay. The results in Table 1 used a final ATP concentration of 10 μM, within the predetermined linear range of the assay, as described in more detail in Section 2.3.5 (Blidner 2007).

Table 1 – Luciferase ATP assay with caged effectors

Sample	Before UVA light exposure (RLU)	After UVA light exposure (RLU)
ATP [10 μM]	7852 ± 438	N/A
γNPE-caged ATP [10 μM]	295 ± 13	5623 ± 394
Base-caged ATP [10 μM] *	1 ± 1.3	4958 ± 266
Unreacted CPR-TP [10 μM]	6 ± 10.9	N/A

*Crude, unpurified product (Blidner unpublished work)

The caged ATP species were co-incubated with free ATP (10 μM final concentrations, 50 μL) to evaluate competitive inhibition. The percentages of ATP activity of the co-incubations, relative to an ATP standard plus buffer that was run in parallel, are shown in Table 2. The γ-phosphate caged ATP reduced the observed luminescent signal, indicating competitive inhibition. Conversely, no statistical difference could be drawn between the free ATP standard and the co-incubation of ATP with base-caged ATP (Blidner 2007).

Table 2 – % of RLU from ATP co-incubated with caged effectors

Sample	2-nitrobenzyl
ATP alone [10 μM]	100.0% ± 32.0%
ATP [10 μM] + γNPE-caged ATP [10 μM]	† 23.0% ± 9.0%
ATP [10 μM] + base-caged ATP [10 μM]	‡ 128.1% ± 12.6%

Symbol † denotes statistical difference between caged-ATP and ATP standard
Symbol ‡ denotes statistical difference between γ-phosphate and base caged ATP
(Student's t-test $p < 0.05$) (Blidner unpublished work)

The results in Table 1 and Table 2 provided support for continuing this work to obtain purified products for characterization and publishable data.

2.2 Experimental Design

This project sought to develop a precise photocaging synthesis process, utilizing base-caged ATP as a model system for caged RNA. As mentioned above, preliminary data suggested that base-caged ATP does exhibit the desired characteristics of bioactivity. However, this data was obtained from crude products without purification or structural characterization. Key issues with the previous protocol included the formation of a triethylammonium salt during the caging synthesis, which proved difficult to remove from the product mixture. Another significant challenge in the prior work was the purification of the caged ATP in order to accurately

characterize the results. Various separation procedures through column chromatography and HPLC were utilized to effectively purify the base-caged ATP. Finally, purified base-caged ATP was utilized to demonstrate caging efficacy and comparative competitive inhibition behavior in a luciferase reporter assay. The experimental design is shown graphically in Figure 10.

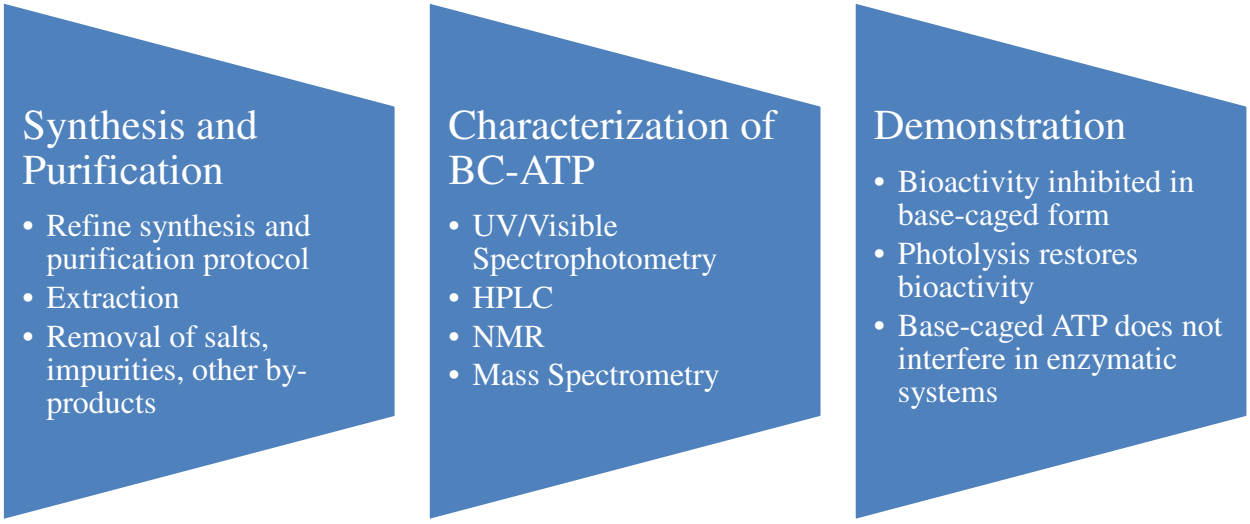

Figure 10 – Project Overview

2.3 Materials and Methods

2.3.1 Base-caged ATP Synthesis

2-nitrobenzylamine (NB-NH_2), triethylamine (TEA), and 6-chloropurine riboside (CPR) were purchased from Sigma Aldrich (St. Louis, MO). 6-Chloropurine riboside-5'-triphosphate (CPR-TP) was purchased from Trilink Biotechnologies (San Diego, CA). TEA is utilized in this organic synthesis as a base, because the nucleophilic aromatic substitution reaction leads to the production of hydrogen chloride (Paquette 2009). The HCl combines with TEA to form triethylammonium chloride, and therefore allows the reaction to proceed to completion upon removal of the hydrogen chloride.

The reaction mixture for synthesizing base-caged ATP was first prepared by dissolving NB-NH_2 (0.040 g) in methanol (150-400 µL) by heating to 60˚C in a water bath. Triethylamine (50 µL) was added to the reaction mixture, along with CPR-TP (1 µmole). Once combined, the reaction mixture was rocked and incubated at 50˚C for 24 hours in a water bath shaker. The reaction scheme is shown in **Figure 11**.

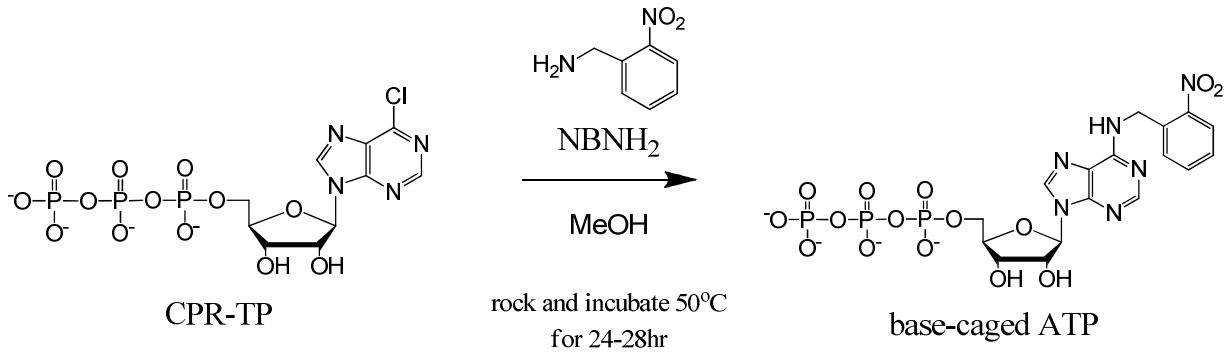

Figure 11 – Synthesis Scheme for Base-Caged ATP
Nitrobenzylamine is dissolved in methanol, and then CPR-TP and triethylamine are added to the reaction mixture. The mixture is rocked and incubated at 50°C for 24 to 28 hours to produce base-caged ATP.

2.3.2 Extraction and Purification

Upon completion of the synthesis, excess NB-NH_2 was separated from the other reaction substituents via liquid-liquid extraction. Dichloromethane (DCM) (MW = 84.93 g/mol, 100 µL) and deionized water (100 µL) were added to the solution and mixed by shaking. The solution was briefly centrifuged, and the aqueous layer was collected. The extraction was repeated twice more with 100 µL of DCM. If chemical analysis indicated that NB-NH_2 remained in the aqueous layer, the liquid-liquid extraction was repeated.

Sodium bicarbonate was then added to the reaction mixture to dissociate the triethylammonium chloride and allow for its removal from the reaction mixture as

triethylammonium bicarbonate (TEAB). The resulting sodium bicarbonate mixture was dried *in vacuo*, re-suspended in methanol and processed via silica gel column chromatography. The sodium bicarbonate was retained by the column and allowed for the separation of base-caged ATP from salt contaminants. Samples were stored at 4˚C and protected from light.

2.3.3 Photolysis

Caged compounds are commonly activated by short, intense exposures to wavelengths of light in the UVA range (315–400 nm) (Forman, Dietrich et al. 2007). Commonly, electron-donating ring substitutions on cage compounds result in a hyperchromatic absorbance shift, or an increase in energy absorbance. This allows photolysis to occur at longer wavelengths that are less damaging to cells or other biological systems (Casey, Blidner et al. 2009).

For this work, photolysis was conducted via transilluminator (TFM-20, UVP Inc., Upland, CA). The transilluminator was used to photolyze BC-ATP and γ-NPE caged ATP samples in 200 µL thin walled PCR Eppendorf tubes at a UVB wavelength of 308 nm with an irradiance of 6.5 mW/cm^2 (Blidner 2007). The total light delivered was 60 J/cm^2. For these *in vitro* experiments, negligible photoeffects of 308 nm exposure were observed, though

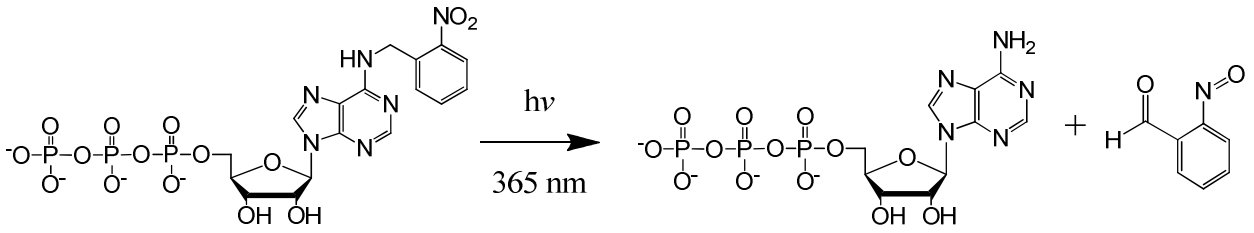

Figure 12 – Photolysis Scheme

this wavelength would have damaging photoeffects *in vivo* (Forman, Dietrich et al. 2007). The photolysis scheme is represented in **Figure 12**.

The quantum yield of the radiation-induced photolysis is the number of caged ATP that photolyze to become free ATP molecules per photon absorbed by the system: Φ = # reactant molecules decomposed / # photons absorbed. The quantum yield of base-caged ATP was determined enzymatically (see Section 2.3.5) by stepping through several time points in photolyzing the caged ATP. Both base-caged ATP and γNPE-caged ATP were photolyzed in this method to determine which caging strategy had the most efficient photolysis.

2.3.4 Characterization

2.3.4.1 UV/Vis Spectrophotometry

Throughout the project, several spectroscopy techniques were used to determine the compositions of samples and evaluate the synthesis and purification of base-caged ATP. Spectrophotometry has been widely used to characterize the absorbance spectra of caged nucleotides and their photoproducts (Walker, Reid et al. 1988). Spectrophotometry of the products and reactants was conducted in the visible and UV range using the Spectronic GENESYS 6 UV-Visible Spectrophotometer (Thermo Scientific) and the spectrophotometer built into the HPLC (Dionex).

2.3.4.2 HPLC

The processed base-caged ATP was analyzed via reverse-phase HPLC (Dionex) on a C18 column at a flow rate of 0.4 mL/min with the solvent conditions shown in **Figure 13.**

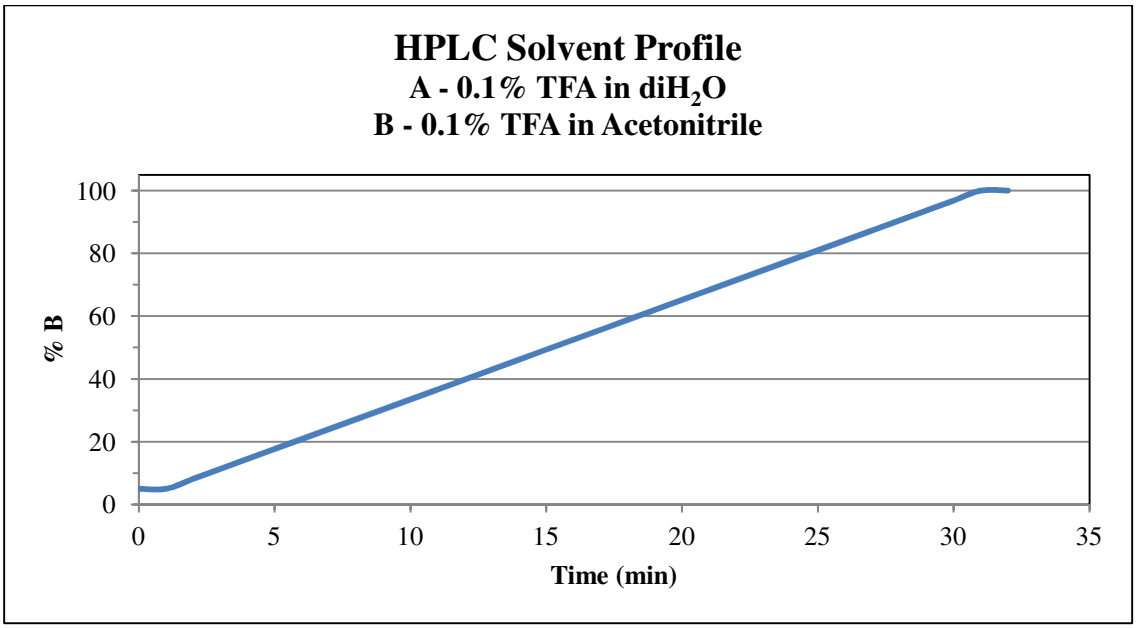

Figure 13 – HPLC reverse phase solvent conditions.
A-0.1% trifluoroacetic acid (TFA) in diH_2O and B-0.1% trifluoroacetic acid (TFA) in acetonitrile.

2.3.4.3 Nuclear Magnetic Resonance Spectroscopy

Nuclear magnetic resonance (NMR) spectroscopy was conducted using ^1H (proton) signals. The solvent for analysis was 100% deuterium oxide (D_2O). Samples were dissolved in 600 µL D_2O and transferred to the NMR tubes. The NMR spectroscopy was conducted using the Bruker AV-400 in the LSU Chemistry Department NMR facility.

2.3.4.4 Mass Spectrometry

Products purified through HPLC and column chromatography were analyzed through electrospray ionization mass spectrometry (ESI-MS) to verify their molecular weights. ESI-MS (negative ion mode) was conducted externally through the LSU Chemistry Department's Agilent 6210 spectrometer.

2.3.5 Enzymatic Demonstration

Base-caged ATP was evaluated in an enzymatic assay to determine the degree of bioactivity in the caged and photoactivated states. As discussed in Section 2.2, it was important to study the inhibited bioactivity of ATP in base-caged form, the efficacy of photolysis in the restoration of bioactivity, and competitive inhibition of base-caged ATP relative to the known inhibitory moieties in enzymatic systems. Both base-caged ATP and γNPE-caged ATP were co-incubated with native ATP, and the experiments were run in parallel to determine the properties of competitive inhibition.

An ENLITEN® ATP Assay System (Promega, Madison, WI) was utilized to quantitatively detect the biological activity of photolyzed base-caged ATP and analyze competitive inhibition in comparison. Native ATP and γ-NPE ATP were utilized for positive controls. rLuciferase/Luciferin (rL/L) reagent was reconstituted according to the manufacturer's instructions. The assay was conducted via Wallac 1420 Multilabel Counter (PerkinElmer, Waltham, MA) in the LSU AgCenter Biotechnology Laboratory (ABL). The Wallac dispenser unit provided automated rL/L addition to the samples on a 96-well white opaque plate, and luminescence was measured in RLUs (relative luminescence unit).

ATP is required for the oxidation of luciferin, which produces luminescence when ATP is hydrolyzed. In the range of 10^{-8} to 10^{-6} M ATP, luminescence of the luciferase assay increases linearly with ATP concentration (Geibel, Barth et al. 2000). ATP concentrations within this range were determined through luminescence measurements. The standard curve for the luciferase assay was established for each run with the luminometer due to the significant variance in luminescence according to temperature and time of storage. The volume of the ATP

standard was small in order for the reaction to favor the forward direction and give accurate RLU output (Lundin 2000). As a standard, 5 μL of ATP solutions (10^{-6}, 10^{-7}, 10^{-8} M ATP in purified water) were mixed with 60 μL of ATP-free water, 10 μL aliquots of luciferase assay solution were automatically injected by the plate reader, and the luminescence was determined (Geibel, Barth et al. 2000). The light emission due to the ATP standard was used to calculate the ratio between RLU and ATP concentration. To verify base-caged ATP concentration as determined by UV/Visible spectrophotometry measurement, 5 μL of the photolyzed base-caged ATP sample solution was mixed with the same ATP-free water and luciferase assay solution volumes, and the luminescence was determined.

The co-incubation experiments required a different protocol using the luminometer. The initial protocol evaluating the competitive inhibition of native ATP by caged ATP species utilized the protocol above, with 5 μL sample volumes, 60 μL of ATP-free water to ensure coverage of the well, 10 μL aliquots of luciferase assay solution were automatically injected into the programmed wells, and after shaking for 1 second, the luminescence readings were taken. After optimization for maximum competitive inhibition of native ATP luminescence by γ-NPE ATP, 7.5 μL of ATP standards were used with 7.5 μL of ATP-free water, and the co-incubations were set up using 7.5 μL of caged ATP plus 7.5 μL of native ATP, 100 uM initial concentrations. The luciferin/luciferase solution was diluted to 1:100 and the injection volume was increased to 60 μL, for a final concentration of 10 uM of each species. Once the luciferin/luciferase solution was injected, the plate was shaken for 3 seconds and the luminescence readings were taken.

CHAPTER 3 – RESULTS

3.1 Characterization

3.1.1 UV/Vis Spectrophotometry

Initial characterization of BC-ATP was based on UV/Visible spectrophotometry and direct mass spectrometry of the purified product. Base-caged ATP has a UV/visible absorbance spectrum that is not only distinct from the primary reactants CPR-TP, NB-NH_2, and TEA, but is also very similar to γ-NPE ATP (Figure 14). The photolyzed BC-ATP spectrum closely correlates to native ATP. Notably, photolyzed BC-ATP and native ATP share a local absorbance maximum at 259 nm, while the peak for caged BC-ATP is red shifted to 268 nm.

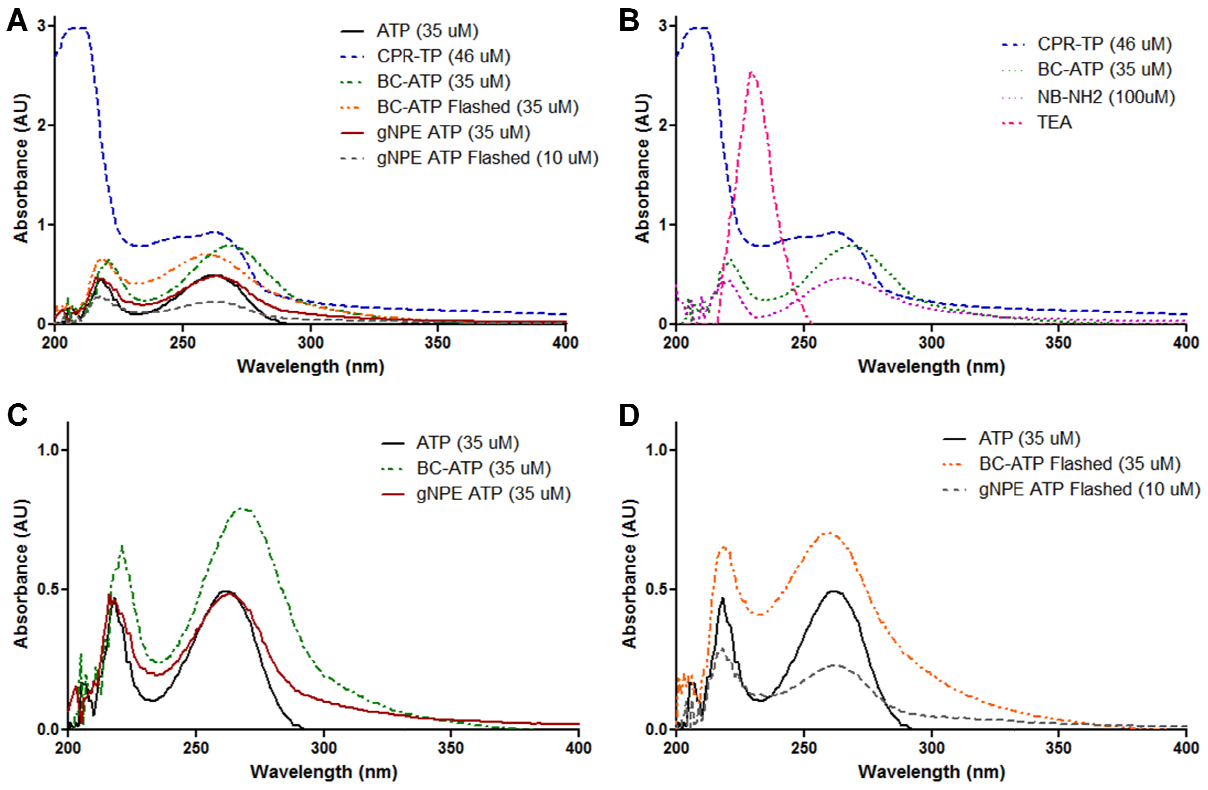

Figure 14 – UV/Visible absorbance spectra.
A. Spectra of native ATP, initial reactant CPR-TP, base-caged ATP, photolyzed BC-ATP, γ-NPE caged ATP, and photolyzed γ-NPE ATP. B. Comparison of reaction materials spectra – CPR-TP, NB-NH2, TEA – and final product BC-ATP. C. Comparison of caged species spectra with native ATP. D. Comparison of photolyzed species spectra with native ATP.

The concentration of BC-ATP was determined indirectly by UV/visible absorbance spectral data. A standard absorbance curve was developed using the known mass, volume, and structure of γ-NPE ATP, from which the concentration of BC-ATP was extrapolated. The extrapolated concentration was then confirmed with luciferase luminescence data that was statistically equivalent for photolyzed BC-ATP and γ-NPE ATP receiving the same irradiance. The absorbance peaks for the associated molecules are shown in **Table 3**.

Table 3 – UV/Vis Absorbance Peaks

Molecule	Absorbance Peak (nm)
Native ATP	258 – 260 [a]
CPR-TP	262 [b]
Base-caged ATP	260 – 265
γNPE caged ATP	259 – 261 [a]
NB-NH_2	220, 260

Absorbance peaks provided by [a] Sigma-Aldrich, [b] TriLink BioTechnologies.

3.1.2 Mass Spectrometry

Mass spectral analysis using negative ion mode MS-ESI was successful in identifying the target base-caged ATP. The mass spectrometry results yielded an exact mass *m/z* of 641.02, corresponding to the elemental composition of $C_{17}H_{21}N_6O_{15}P_3$ within 0.01 ppm (theoretical *m/z* 641.03). Also seen in the mass spectrum were values corresponding to base-caged adenosine diphosphate (*m/z* 561.05). In both caged and photolyzed base-caged ATP sample, native ATP was identified at *m/z* = 505.98, indicating photolysis occurred despite protecting BC-ATP from light. These molecular structures and their exact masses are shown in **Figure 15**, and the mass spectrum of base-caged ATP is shown in **Figure 16**.

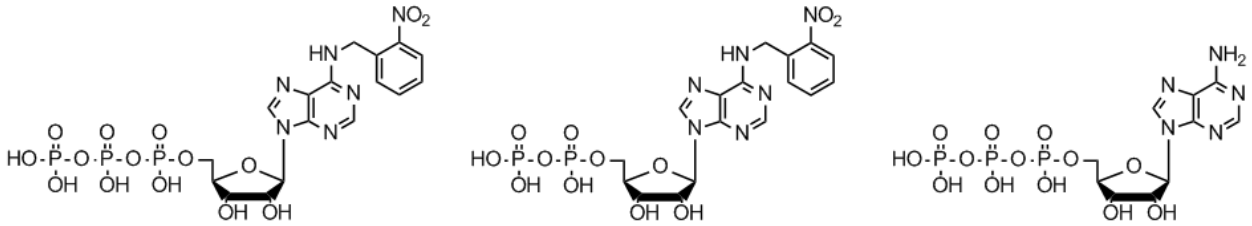

Figure 15 – Exact Masses for A. Base-caged ATP, B. Base-caged adenosine diphosphate, C. Native ATP

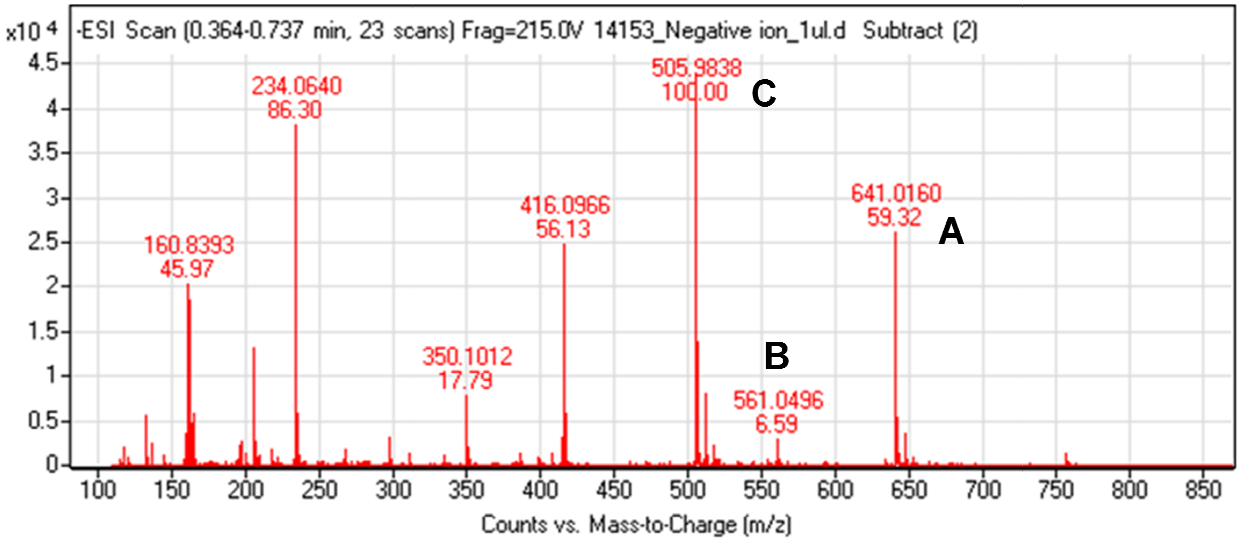

Figure 16 – Mass Spectrum of BC-ATP: A. Base-caged ATP, B. base-caged adenosine diphosphate, C. native ATP.

The electrospray ionization conditions applied to base-caged ATP during mass spectral analysis can lead to the uncaging of the molecule. In addition, some of the caged products were hydrolyzed to base-caged adenosine diphosphate under the ESI conditions. These results do not necessarily reflect an impure product, but rather the conditions of the analysis.

3.1.3 HPLC

Chromatographic analysis via HPLC revealed that the elution time of the base-caged ATP more closely followed NB-NH_2 rather than native ATP, shown in **Figure 17**. The primary signal for BC-ATP occurred at about 11 minutes, while native ATP eluted from the column at about 5 minutes. The chromatograms demonstrate the shift in polarity of the caged ATP from

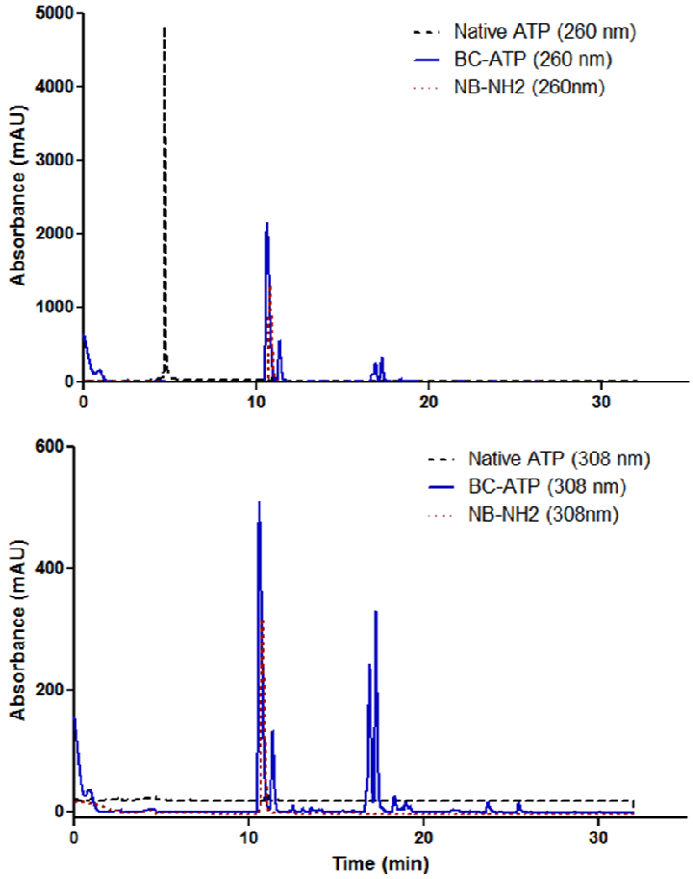

Figure 17 – HPLC Chromatogram of Native ATP, BC-ATP, and NB-NH_2 at 260nm and 308nm.

native ATP due to the addition of the nitrobenzylamine cage molecule. Closer inspection of the caged and flashed BC-ATP chromatograms revealed important trends. **Figure 18** clearly shows the absence of the native ATP peak for base-caged ATP, while the photolyzed BC-ATP has the peak that closely follows the native ATP peak at about 4.6 minutes.

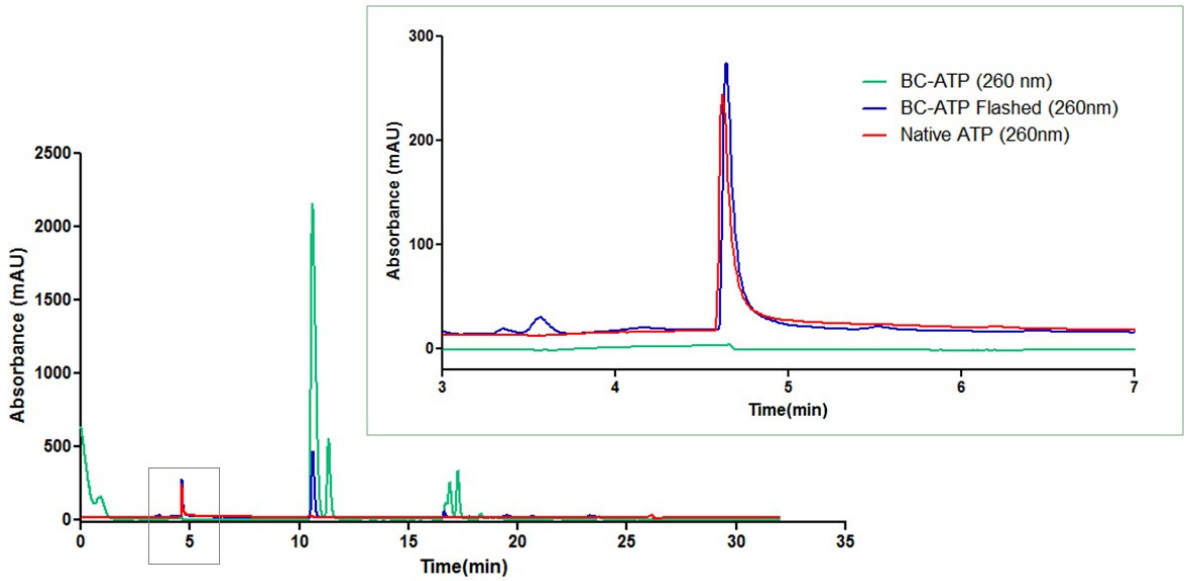

Figure 18 – HPLC Chromatogram of BC-ATP (caged and flashed) and Native ATP at 260nm

The chromatogram for the 308nm detector is shown in **Figure 19**. Here, the flashed BC-ATP closely follows the native ATP signal. During the course of the HPLC analyses, it was discovered that the native ATP peak integration actually decreased with increased photolyzation time. This was detected by studying the elution peak integration trends shown in **Figure 20**.

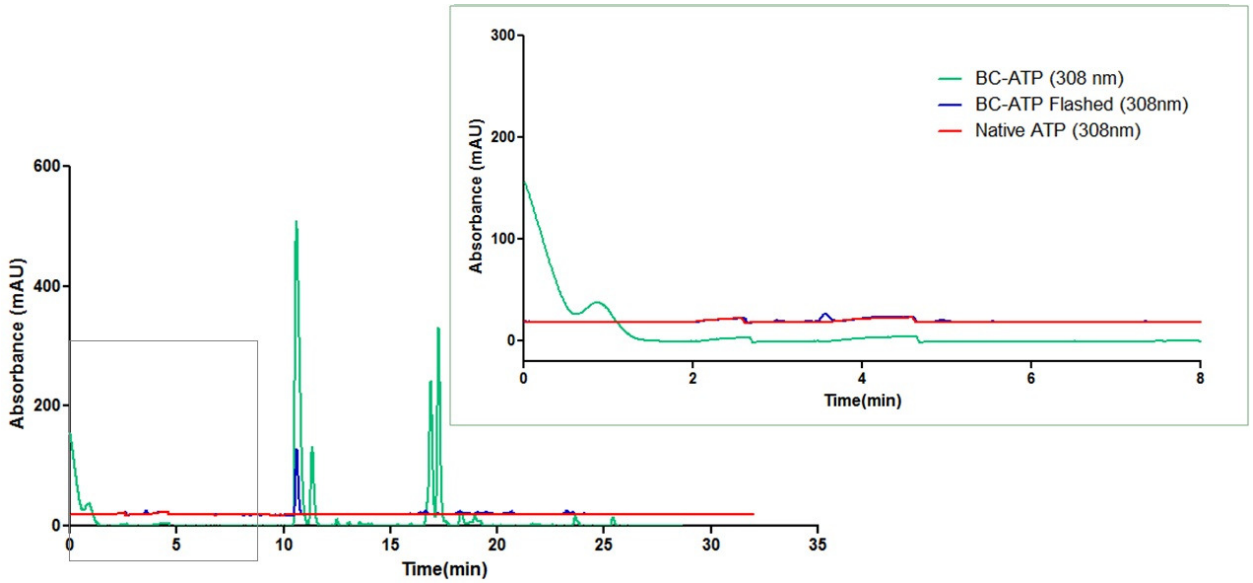

Figure 19 – HPLC Chromatogram of BC-ATP (caged and flashed) and Native ATP at 308nm

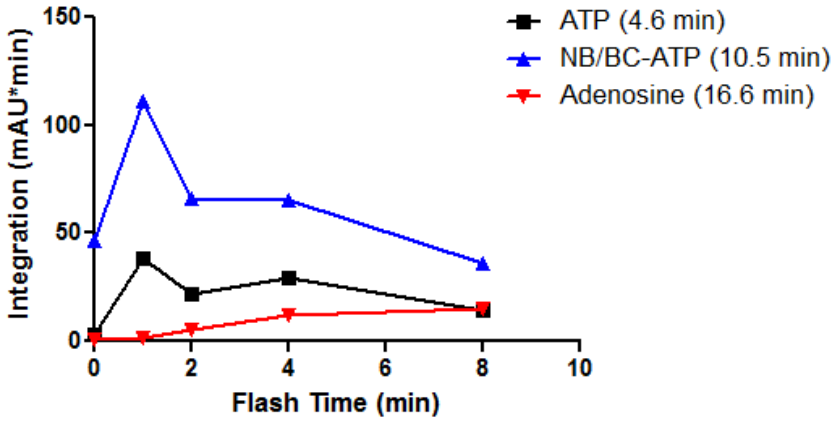

Figure 20 – HPLC Peak Integrations at 260nm

The elution peak integration trends show that increased photolyzation time led to the possible degradation of base-caged ATP into an adenosine product. The identity of the adenosine product was confirmed by liquid chromatography–mass spectrometry (LC-MS) conducted under the same HPLC conditions, shown in **Figure 21** and **Figure 22**.

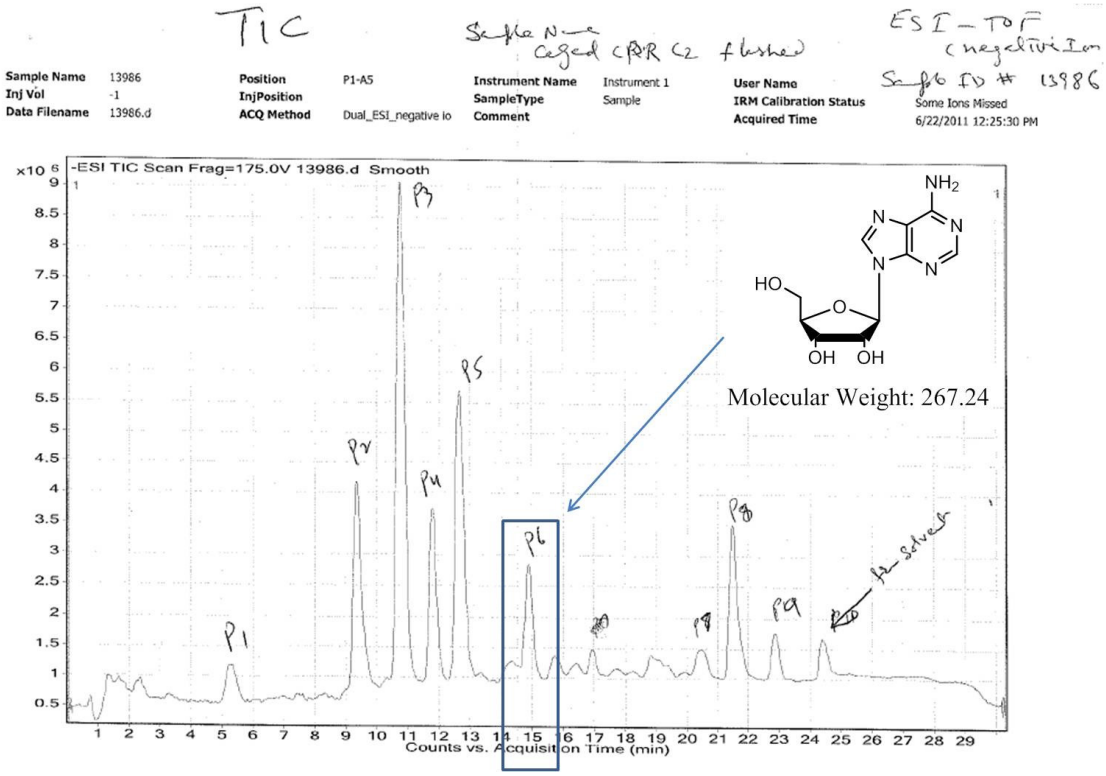

Figure 21 – LC-MS Chromatogram Highlighting Free Adenosine

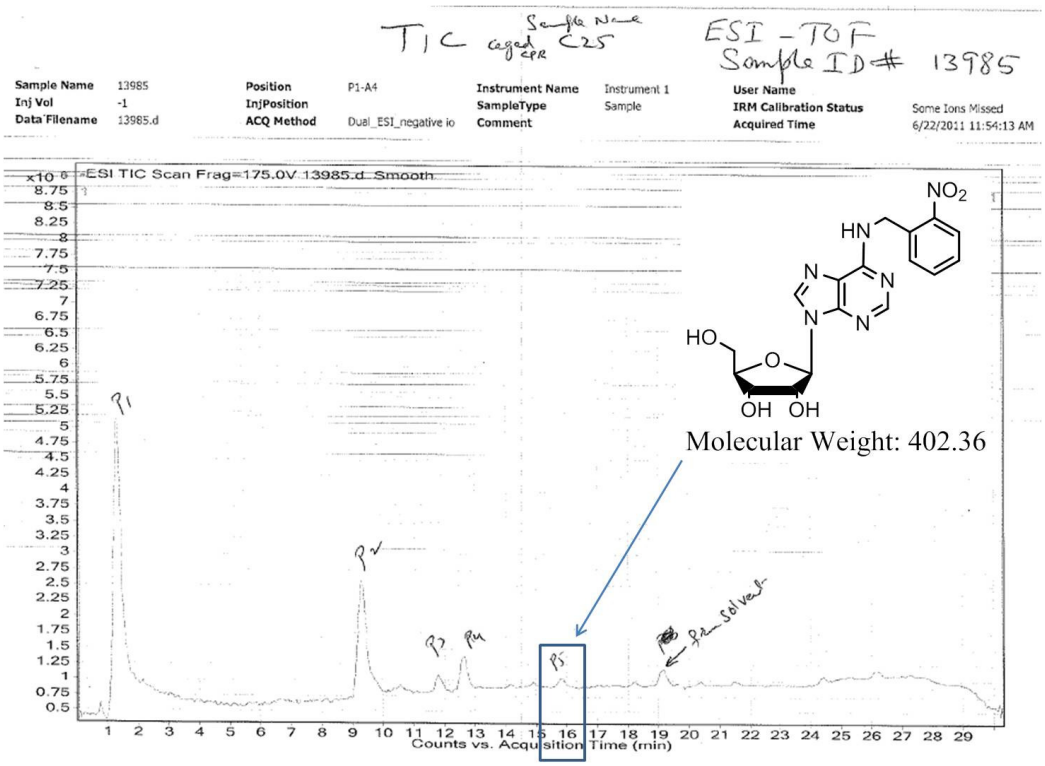

Figure 22 – LC-MS Chromatogram Highlighting Caged Adenosine

Although LC-MS was conducted on a slightly different reaction product, the overlapping elution time highly suggests that either free adenosine or caged adenosine elute from the flashed BC-ATP column at 16.6 minutes. Therefore, referring back to **Figure 20**, it is likely that the continued photolysis of base-caged ATP at a wavelength of 308nm led to the degradation and loss of phosphate groups. Shorter photolysis time and a longer, lower energy wavelength UV light may resolve this degradation issue in the future.

3.1.4 Nuclear Magnetic Resonance Spectroscopy

To provide further evidence of the proposed BC-ATP structure we sought to analyze it by NMR spectroscopy. Purification of the sample was unable to fully separate triethylamine from the base-caged ATP despite many attempts to separate the two species (**Figure 23**). However,

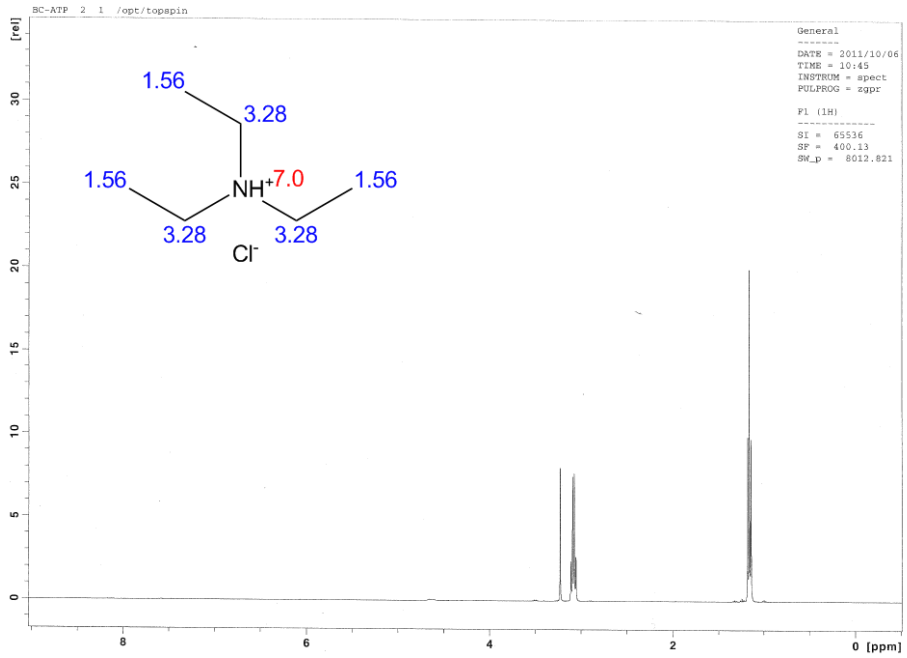

Figure 23 – ^{1}H NMR Spectrum for BC-ATP triethylammonium salt.
The spectrum is dominated by triethylammonium salt in the sample.

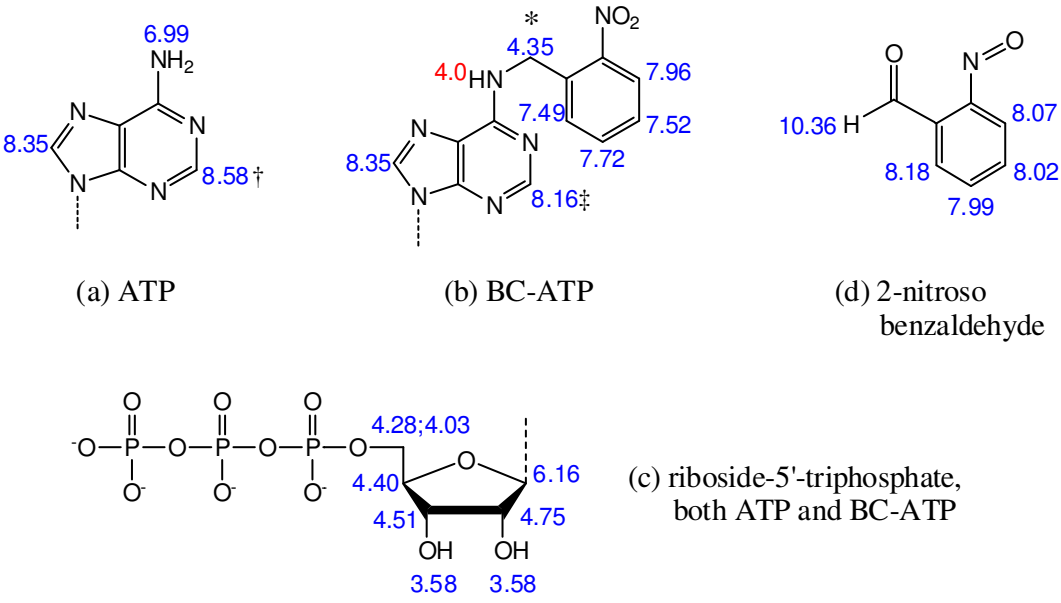

Figure 24 – ChemDraw Predicted NMR ^{1}H Shifts for (a) ATP, (b) BC-ATP, and (d) 2-nitrosobenzaldehyde (ppm)
A. Native ATP has the unique signal of 8.58 ppm for the proton at †. B. Base-caged ATP is expected to have the 4.35 ppm signal for the -CH_2 protons (*) and the 8.16 ppm signal for the proton at ‡. D. The predicted proton shifts for 2-nitrosobenzaldehyde.

ATP analogues are often supplied as triethylammonium salts, so this association is not expected to have a significant impact on biological performance (Google search “atp triethylammonium salt”). Additionally, triethylamine has been utilized in caged ATP synthesis since the beginning of its existence (Kaplan, Forbush et al. 1978).

Although the N^6 proton of adenosine would structurally appear to be a good indicator of cage status for base-caged ATP, its signal is too difficult to predict or identify on the NMR spectrum. Instead, the -CH_2 protons on the carbon between the nitrobenzyl group and ATP were

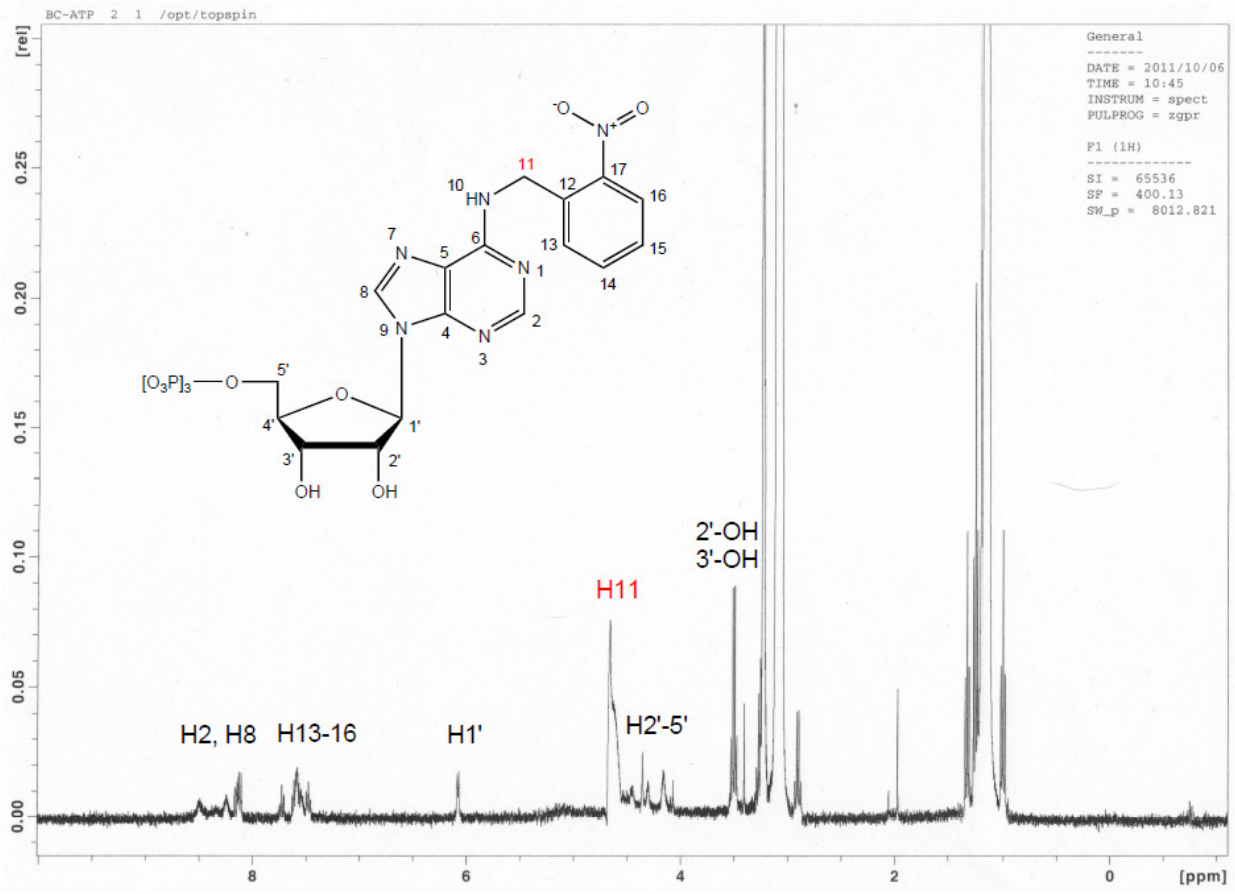

Figure 25 – ^{1}H NMR Spectrum of BC-ATP in D_2O.
Inspection of the spectrum reveals the expected base-caged ATP signals. Most notable is the strong signal at approximately 4.5 which closely corresponds to the expected signal from the -CH_2 protons at carbon 11.

used as markers to evaluate the sample compositions as shown by the predicted NMR spectra shown in **Figure 24**. This proton location is designated "H11" in **Figure 25**.

Analysis of the "zoomed-in" NMR spectrum of base-caged ATP (**Figure 25**) reveals the signal pattern that closely corresponds to the expected proton shifts in **Figure 24**. Most notable is the strong signal at approximately 4.5 which closely corresponds to the expected signal from the -CH_2 protons. The ribose, purine, and benzyl protons are also distinct and exhibit the expected shifts. Native ATP and the photolysis product 2-nitrosobenzaldehyde are not detectable in the sample as determined by the lack of signals at 6.99 and 10.36 ppm, respectively.

3.2 Enzymatic Demonstration – Luciferase Assay

The recombinant firefly luciferase assay was utilized initially to validate the quantification of base-caged ATP, and then to evaluate its biological activity performance prior to and following photolysis. Due to the inherent variability of the luciferase assay, all data are normalized according to ATP standards run with each experiment as per supplier specifications. As shown in **Figure 26**, base-caged ATP demonstrated caged and photolyzed luminescence that is comparable to γ-NPE ATP. However, caged BC-ATP showed a 3.11% level of leak that could be attributed to processing without buffer solution. This is a statistically significant difference from the leak exhibited by γ-NPE ATP ($P < 0.001$). It is also important to note that the BC-ATP precursor reactant CPR-TP has negligible luminescence, indicating that the initial ATP analog compound has no biological activity.

Both caged and photolyzed samples of BC-ATP and γ-NPE ATP were co-incubated with native ATP to evaluate the competitive inhibition of luminescence activity of native ATP by the

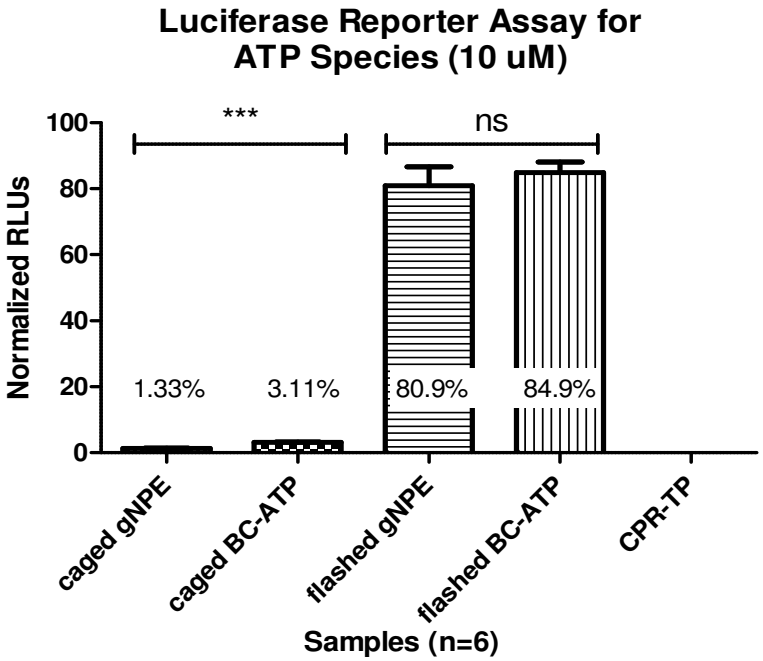

Figure 26 – Luciferase Reporter Assay for Caged vs Flashed ATP
Normalized relative luminescence units (RLUs) comparison of BC-ATP, γ-NPE ATP and CPR-TP. Caged BC-ATP shows a 3.11% leak. Photolyzed BC-ATP and γ-NPE ATP show statistically equivalent luminescence. CPR-TP exhibits negligible luminescence.

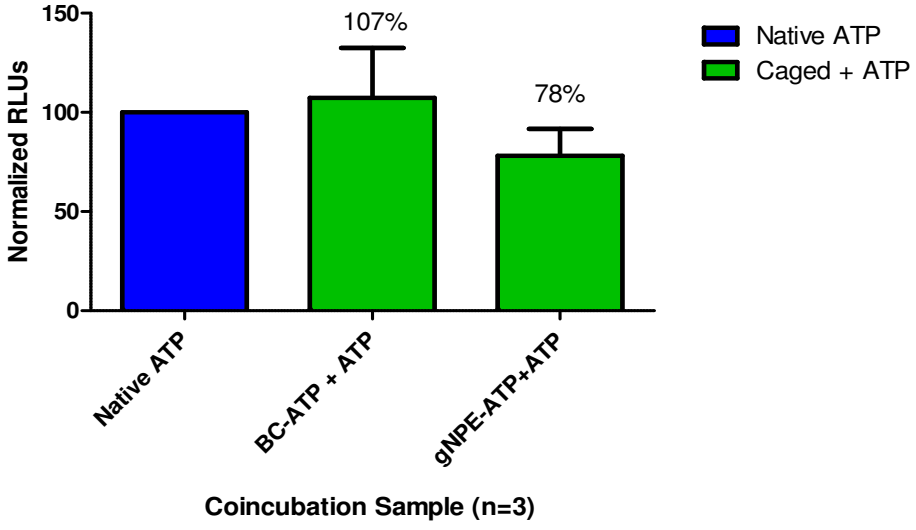

Figure 27 – Evaluation of Competitive Inhibition with Co-incubations of Caged ATP and Native ATP.
All species 10 μM final concentrations. Native ATP was competitively inhibited by γ-NPE caged-ATP by 22% (or 78% luminescence). No inhibition was observed for the co-incubation of native ATP with base-caged ATP.

caged molecules. First, the luciferase assay was optimized using native ATP and γ-NPE caged-ATP co-incubations to establish the conditions under which competitive inhibition was greatest. The resulting protocol with 10 μM final concentrations was outlined in **Section 2.3.5**. The maximum repeatable competitive inhibition of native ATP by caged γ-NPE ATP was 78% luminescence, or 22% inhibition of native ATP in solution, seen in **Figure 27**. The co-incubation of native ATP with base-caged ATP shows some leak luminescence, but no competitive inhibition. The flashed co-incubations for BC-ATP and γ-NPE ATP were statistically equivalent (data not shown).

CHAPTER 4 – DISCUSSION

In summary, we have characterized a novel form of photocaged ATP by attaching the cage molecule to the N^6 position of adenosine, and we have demonstrated that it exhibits activity as a photocaged substrate. First, the base-caged ATP shows 3.11% luminescence activity in the uninduced form and, upon exposure to 308 nm radiation, the biological activity of ATP is restored to a level of luminescence statistically equivalent to that of photolyzed γ-NPE ATP.

Secondly, the utilization of base-caged ATP results in significant improvement in competitive inhibition with native ATP in powering an enzymatic system. The chief problem of competitive inhibition by the standard γ-NPE ATP in a variety of enzymatic studies, as discussed in **Section 1.5.1**, may be largely resolved with base-caged ATP. While γ-NPE ATP in solution with native ATP results in an average of 22% inhibition, base-caged ATP exhibits no such competitive inhibition. Further research into the kinetics of base-caged ATP- and photolyzed BC-ATP-binding to an enzymatic molecule is required before an exact comparison can be made to the examples of competitive inhibition seen in literature (Forbush 1984; Sleep, Herrmann et al. 1994; Thirlwell, Corrie et al. 1994; Thirlwell, Sleep et al. 1995; Broustovetsky, Bamberg et al. 1997; Higuchi, Muto et al. 1997). These studies characterized the competitive inhibition seen

Table 4 – Inhibitor Dissociation Constants for γ-NPE ATP

Investigator	**System**	**K_i**
Thirlwell *et al*. 1994	actomyosin ATPase	1-2mM
Sleep *et al*. 1994	myofibrils and actomyosin subfragment 1	1.6-1.8mM
Higuchi *et al*. 1997	kinesin and microtubules	1.5 mM
Broustovetsky *et al*. 1997	mitochondrial ADP/ATP carrier (AAC)	5 μM

with γ-NPE ATP by determining K_i, the dissociation constant for the inhibitor. The inhibitor dissociation constants for studies utilizing γ-NPE ATP are shown in **Table 4**.

In addition to the synthesis and characterization of this novel photocaged ATP species, the enzymatic results support the hypothesis that alkylating the N^6 position of ATP with the cage molecule prevents the enzyme-substrate binding from occurring prior to photolysis. Since firefly luciferase and numerous ATP-dependent enzymes require access to the N^6 position for nucleotide recognition and binding, base-caged ATP effectively blocks the N^6 amino proton from participating in hydrogen-bond binding. The hydrogen-bond obstruction is achieved in two modes: not only is one of the protons removed in the synthesis of base-caged ATP, reducing the availability of protons by 50%, but the cage molecule also introduces steric hindrance to prevent enzyme binding to the remaining N^6 proton. By physically blocking the binding of base-caged ATP to the enzyme, competitive inhibition is eliminated.

CHAPTER 5 – CONCLUSION

5.1 Conclusion

The synthesis of base-caged ATP yielded a product which was purified and then fully characterized and confirmed by a combination of analytical chemistry techniques. By caging ATP at the N^6 position of adenosine, biological activity is first prevented in the uninduced form, and exposure to 308 nm radiation induces the biological activity of ATP, suggesting that a photocaged form of ATP has indeed been synthesized. In addition, competitive inhibition has been minimized in the luciferase assay in comparison to γ-NPE ATP. This novel version of caged ATP should allow for kinetic studies of ATP-dependent enzymatic systems without the complication of competitive inhibition shown by γ-NPE ATP.

5.2 Implications for Future Work

Beyond kinetic enzymatic studies, base-caged ATP has broad implications for its use in exerting spatial-temporal control over a substrate. The protocol for synthesizing base-caged ATP can now be applied to achieve a base-caged oligonucleotide using the convertible nucleoside approach (Allerson, Chen et al. 1997). This method initially site-specifically incorporates into RNA synthesis a nucleoside analog with a leaving group on the nucleobase. The full length RNA is treated with a nucleophile to displace the leaving group and yield the desired nucleoside with an exocyclically tethered alkylamine, the photolabile cage molecule (Allerson, Chen et al. 1997). By using the convertible nucleoside method, CPR-TP would be incorporated into the oligonucleotide in the positions where caged adenosine is desired, and then the RNA would be treated with 2-nitrobenzylamine to form the caged oligonucleotide. Sites for

photocaging could then be experimentally optimized in order to determine the minimal number of cage molecules to prevent leak (incomplete suppression of bioactivity while caged) while maximizing quantum yield. The quantum yield, or relationship between the required light energy and the number of bound cage compounds, would then need to be determined for the caged oligonucleotide. Once this technique is successful, site-specific base-caged oligonucleotides will be readily available to utilize in such systems as RNA interference with a base-caged small interfering RNA. A base-caged siRNA would be particularly beneficial in achieving complex tissue cultures requiring spatio-temporally directed gene knockdown.

More advanced studies would apply base-caged siRNA technology to cellular and *in vivo* model systems. One possible study would utilize a cellular model of musculoskeletal differentiation whereby microRNAs are blocked at certain locations and times with photoactivatable oligonucleotides, achieving spatial and temporal control in directed tissue development *in vitro*. Similarly, caged siRNAs could conceivably be introduced intravenously for activation in a specific tissue such as an open wound where musculoskeletal cell growth would be directed by a UV light application programmed for optimized healing. This approach could also be used to complement cancer therapies by knocking down various oncogenes and other gene markers associated with poor prognosis.

REFERENCES

Allerson, C. R., S. L. Chen, et al. (1997). "A chemical method for site-specific modification of RNA: The convertible nucleoside approach." Journal of the American Chemical Society **119**(32): 7423-7433.

Blidner, R. A. (2007). Base-Caged ATP: an Alternative to γ–Phosphate Caged ATP. Engineering a Photo-Control Mechanism for RNA Interference. Baton Rouge, Louisiana State University**:** 123-134.

Blidner, R. A. (2007). Engineering a Photo-Control Mechanism for RNA Interference. Baton Rouge, Louisiana State University.

Breslow, R. and R. Xu (1993). "Recognition and Catalysis in Nucleic-Acid Chemistry." Proceedings of the National Academy of Sciences of the United States of America **90**(4): 1201-1207.

Broustovetsky, N., E. Bamberg, et al. (1997). "Biochemical and physical parameters of the electrical currents measured with the ADP/ATP carrier by photolysis of caged ADP and ATP." Biochemistry **36**(45): 13865-13872.

Casey, J. P., R. A. Blidner, et al. (2009). "Caged siRNAs for Spatiotemporal Control of Gene Silencing." Molecular Pharmaceutics **6**(3): 669-685.

Chaulk, S. G. and A. M. MacMillan (2007). "Synthesis of oligo-RNAs with photocaged adenosine 2'-hydroxyls." Nat Protoc **2**(5): 1052-1058.

Chen, J. F., E. M. Mandel, et al. (2006). "The role of microRNA-1 and microRNA-133 in skeletal muscle proliferation and differentiation." Nature Genetics **38**(2): 228-233.

Conti, E., N. P. Franks, et al. (1996). "Crystal structure of firefly luciferase throws light on a superfamily of adenylate-forming enzymes." Structure **4**(3): 287-298.

Esquela-Kerscher, A. and F. J. Slack (2006). "Oncomirs - microRNAs with a role in cancer." Nature Reviews Cancer **6**(4): 259-269.

Ferentz, A. E., T. A. Keating, et al. (1993). "Synthesis and Characterization of Disulfide Cross-Linked Oligonucleotides." Journal of the American Chemical Society **115**(20): 9006-9014.

Ferentz, A. E. and G. L. Verdine (1992). "Aminolysis of 2'-Deoxyinosine Aryl Ethers - Nucleoside Model Studies for the Synthesis of Functionally Tethered Oligonucleotides." Nucleosides & Nucleotides **11**(10): 1749-1763.

Fire, A., S. Q. Xu, et al. (1998). "Potent and specific genetic interference by double-stranded RNA in Caenorhabditis elegans." Nature **391**(6669): 806-811.

Forbush, B. (1984). "Na+ Movement in a Single Turnover of the Na Pump." Proceedings of the National Academy of Sciences of the United States of America-Biological Sciences **81**(17): 5310-5314.

Forman, J., M. Dietrich, et al. (2007). "Photobiological and thermal effects of photoactivating UVA light doses on cell cultures." Photochemical & Photobiological Sciences **6**(6): 649-658.

Geibel, S., A. Barth, et al. (2000). "P-3-[2-(4-hydroxyphenyl)-2-oxo]ethyl ATP for the rapid activation of the Na+,K+-ATPase." Biophysical Journal **79**(3): 1346-1357.

Givens, R., M. B. Kotala, et al. (2005). Mechanistic Overview of Phototriggers and Cage Release, Wiley-VCH Verlag GmbH & Co. KGaA.

Givens, R. S., J. F. W. Weber, et al. (1998). [1] New photoprotecting groups: Desyl and p-hydroxyphenacyl phosphate and carboxylate esters. Methods in Enzymology. M. Gerard, Academic Press. **Volume 291:** 1-29.

Gregory, R. I., T. P. Chendrimada, et al. (2005). "Human RISC couples microRNA biogenesis and posttranscriptional gene silencing." Cell **123**(4): 631-640.

Gropp, T., N. Brustovetsky, et al. (1999). "Kinetics of electrogenic transport by the ADP/ATP carrier." Biophysical Journal **77**(2): 714-726.

Hamad-Schifferli, K., J. J. Schwartz, et al. (2002). "Remote electronic control of DNA hybridization through inductive coupling to an attached metal nanocrystal antenna." Nature **415**(6868): 152-155.

Hartwell, L. H., L. Hood, et al. (2008). Genetics: From Genes to Genomes. New York, NY, McGraw Hill.

He, L. and G. J. Hannon (2004). "MicroRNAs: small RNAs with a big role in gene regulation." Nat Rev Genet **5**(7): 522-531.

Higuchi, H., E. Muto, et al. (1997). "Kinetics of force generation by single kinesin molecules activated by laser photolysis of caged ATP." Proceedings of the National Academy of Sciences of the United States of America **94**(9): 4395-4400.

Hobartner, C. and S. K. Silverman (2005). "Modulation of RNA tertiary folding by incorporation of caged nucleotides." Angew Chem Int Ed Engl **44**(44): 7305-7309.

Kaplan, J. H., B. Forbush, et al. (1978). "Rapid Photolytic Release of Adenosine 5'-Triphosphate from a Protected Analog - Utilization by Na-K Pump of Human Red Blood-Cell Ghosts." Biochemistry **17**(10): 1929-1935.

Knowles, J. R. (1980). "Enzyme-Catalyzed Phosphoryl Transfer-Reactions." Annual Review of Biochemistry **49**: 877-919.

Lee, R. T., J. L. Denburg, et al. (1970). "Substrate-binding properties of firefly luciferase. II. ATP-binding site." Arch Biochem Biophys **141**(1): 38-52.

Lundin, A. (2000). "Use of firefly luciferase in ATP-related assays of biomass, enzymes, and metabolites." Bioluminescence and Chemiluminescence, Pt C **305**: 346-370.

Mack, G. S. (2007). "MicroRNA gets down to business." Nature Biotechnology **25**(6): 631-638.

Mao, L., Y. Wang, et al. (2004). "Molecular determinants for ATP-binding in proteins: a data mining and quantum chemical analysis." J Mol Biol **336**(3): 787-807.

Mayer, G. and A. Heckel (2006). "Biologically active molecules with a "light switch"." Angewandte Chemie-International Edition **45**(30): 4900-4921.

Monroe, W. T., M. M. McQuain, et al. (1999). "Targeting expression with light using caged DNA." Journal of Biological Chemistry **274**(30): 20895-20900.

Paquette, L. A. (2009). Encyclopedia of reagents for organic synthesis. Hoboken, N.J., Wiley.

Rhim, C., D. A. Lowell, et al. (2007). "Morphology and ultrastructure of differentiating three-dimensional mammalian skeletal muscle in a collagen gel." Muscle & Nerve **36**(1): 71-80.

Shah, S., S. Rangarajan, et al. (2005). "Light activated RNA interference." Angewandte Chemie-International Edition **44**(9): 1328-1332.

Sleep, J., C. Herrmann, et al. (1994). "Inhibition of ATP binding to myofibrils and acto-myosin subfragment 1 by caged ATP." Biochemistry **33**(20): 6038-6042.

Takahashi, T., T. Ogasawara, et al. (2007). "Three-dimensional microenvironments retain chondrocyte phenotypes during proliferation culture." Tissue Engineering **13**(7): 1583-1592.

Thirlwell, H., J. E. T. Corrie, et al. (1994). "Kinetics of Relaxation from Rigor of Permeabilized Fast-Twitch Skeletal Fibers from the Rabbit Using a Novel Caged-Atp and Apyrase." Biophysical Journal **67**(6): 2436-2447.

Thirlwell, H., J. A. Sleep, et al. (1995). "Inhibition of unloaded shortening velocity in permeabilized muscle fibres by caged ATP compounds." J Muscle Res Cell Motil **16**(2): 131-137.

Walker, J. W., G. P. Reid, et al. (1988). "Photolabile 1-(2-Nitrophenyl)Ethyl Phosphate-Esters of Adenine-Nucleotide Analogs - Synthesis and Mechanism of Photolysis." Journal of the American Chemical Society **110**(21): 7170-7177.

Winter, J., S. Jung, et al. (2009). "Many roads to maturity: microRNA biogenesis pathways and their regulation." Nat Cell Biol **11**(3): 228-234.

Yi, R., Y. Qin, et al. (2003). "Exportin-5 mediates the nuclear export of pre-microRNAs and short hairpin RNAs." Genes & Development **17**(24): 3011-3016.

APPENDIX A - BASE-CAGED ATP SYNTHESIS PROTOCOL

BC-ATP Reaction

1. Dissolve 0.04 g $NBNH_2$ in 150-400 uL methanol in a reaction tube. Heat using hot plate if needed.
2. Add 50 uL triethylamine (TEA).
3. Add 16.6 uL of 10mM (1.67 umole) CPR-TP.
4. Rock and incubate overnight (24-28 hours) at 50˚ C.
5. Evaporate MeOH (BP = 64.7 ˚C)
6. Refrigerate until the next step.

Liquid-liquid Extraction – Conduct in a darkened fume hood

1. Pipette into 1.5 mL microcentrifuge tube: 100 uL DI water and 100 uL dichloromethane (DCM).
2. Pipette caged ATP reaction mixture into the centrifuge tube.
3. Close the tube and shake.
    - Aqueous layer: base-caged ATP, translucent and clear
    - Organic layer: nitrobenzylamine, orange
4. Centrifuge for 3-5 minutes. Extract aqueous layer.
5. Complete three rounds of L/L extraction, adding 50 uL DCM to the aqueous layer from the previous extraction.
6. If the aqueous layer is still reddish in color, complete additional L/L extractions until the aqueous layer is clear.

Column Chromatography Purification – Conduct in a darkened room

1. Add sodium bicarbonate to remove triethyl ammonium salt.
2. Rotovap to dryness (high vacuum 0.001 mm Hg). Resuspend in methanol.
3. Prepare a column with a slurry of silica gel and methanol. Pack a 10mL column so that it is 75-80% silica gel.
4. Add sample and run two column volumes with methanol. Sodium bicarbonate will stay at the top of the column, BC-ATP will stay on the column with methanol, and $NB\text{-}NH_2$ and other contaminants will elute with methanol.
5. Run column with diH_2O to elute BC-ATP.
6. Collect diH_2O fraction and protect from light.
7. Rotovap and resuspend to required concentration.

APPENDIX B - LUCIFERASE PROTOCOL

ENLITEN® ATP Assay System (Promega) measured via Wallac 1420 Multilabel Counter (PerkinElmer) in the LSU AgCenter Biotechnology Laboratory (ABL).

Preparation of assay

1. Reconstitute rLuciferase/Luciferin (rL/L) reagent according to the manufacturer's instructions.
2. Prepare rL/L buffer solution with dH_2O:
    a. 10mM Tris
    b. 0.1mM EDTA
    c. 25 mM $MgCl_2$
    d. Adjust to pH 7.5 with acetic acid.
3. Prepare 1:10 or 1:100 dilutions of rL/L reagent using the rL/L buffer solution as diluent.
4. Aliquot per usage requirements to minimize freeze-thaw cycles.
5. Use 96-well white opaque plate for assay.

Single Sample Luminescence

1. Set plate reader program to auto-inject 10 µL of luciferase assay solution into each well.
2. For ATP Standards (10^{-6}, 10^{-7}, 10^{-8} M ATP in purified water), place 5 µL of ATP standard solutions in designated wells with 60 µL of ATP-free water each.
3. For caged and flashed samples, place 5 µL of sample in well with 60 µL of ATP-free water.
4. Run Wallac protocol "Luminescence ATP (2)" in "by well" measurement mode

Co-Incubation Sample Luminescence

1. Set plate reader program to auto-inject 60 µL of luciferase assay solution into each well.
2. For ATP Standards (10^{-5}, 10^{-6}, 10^{-7} M ATP in purified water), place 7.5 µL of ATP standard solutions in designated wells with 7.5 µL of ATP-free water each.
3. For caged and flashed co-incubations, place 7.5 µL of sample in well with 7.5 µL of native ATP, 100 uM initial concentrations.
4. Run Wallac protocol "Luminescence ATP (2)" in "by well" measurement mode

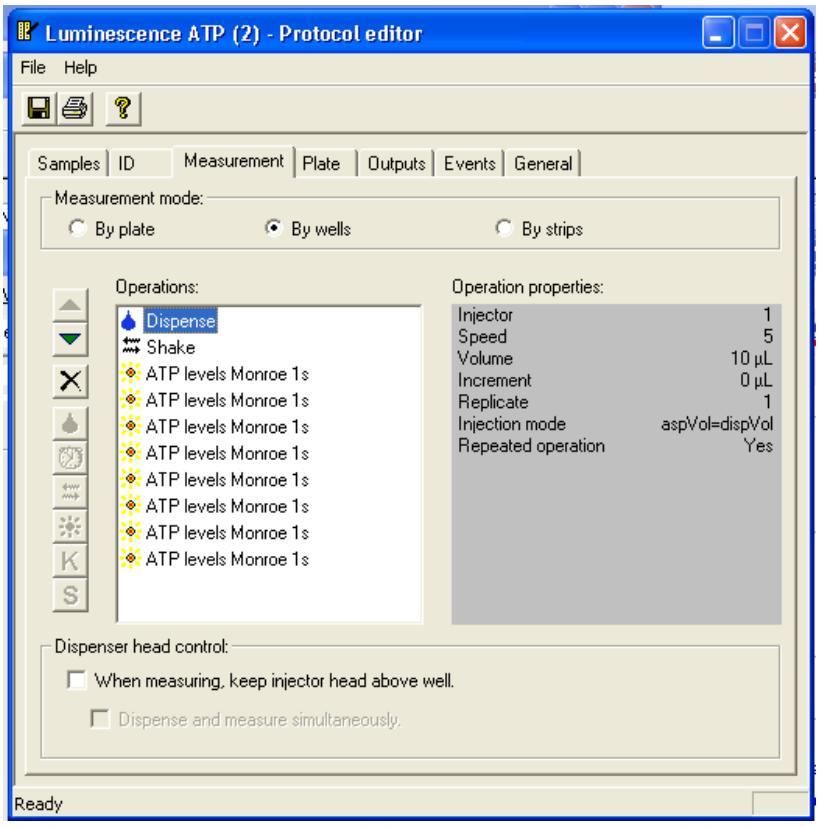
Luminescence ATP (2) - Protocol editor
File Help
Samples ID Measurement Plate Outputs Events General
Measurement mode:
By plate By wells By strips
Operations:
Dispense
Shake
ATP levels Monroe 1s
ATP levels Monroe 1s
ATP levels Monroe 1s
ATP levels Monroe 1s
ATP levels Monroe 1s
ATP levels Monroe 1s
ATP levels Monroe 1s
ATP levels Monroe 1s
Operation properties:
Injector 1
Speed 5
Volume 10 µL
Increment 0 µL
Replicate 1
Injection mode aspVol=dispVol
Repeated operation Yes
Dispenser head control:
When measuring, keep injector head above well.
Dispense and measure simultaneously.
Ready

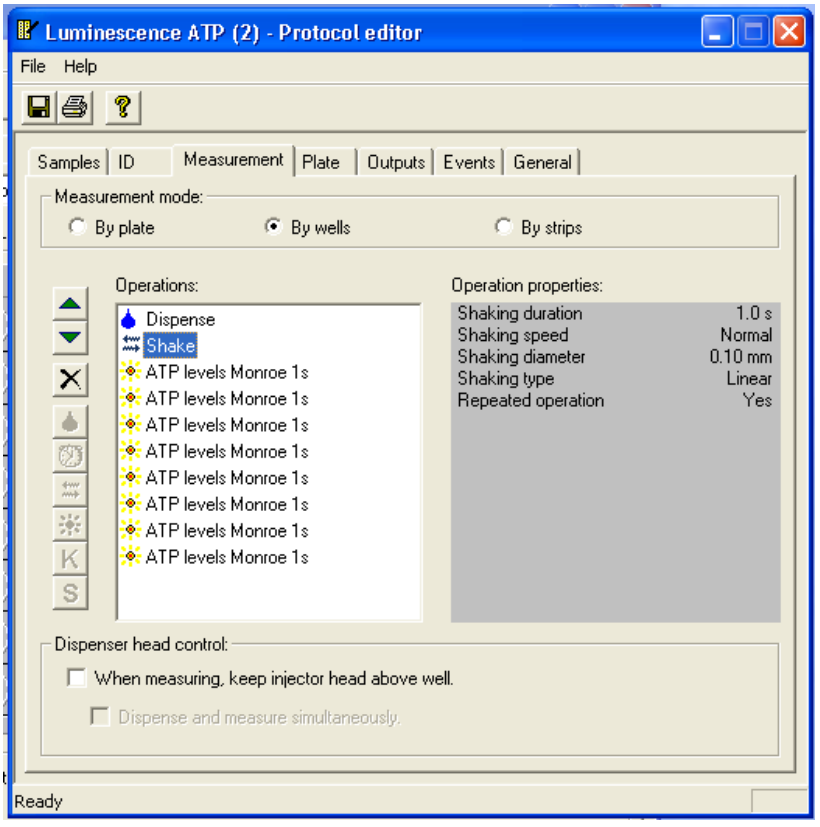
Luminescence ATP (2) - Protocol editor
File Help
Samples ID Measurement Plate Outputs Events General
Measurement mode:
By plate By wells By strips
Operations:
Dispense
Shake
ATP levels Monroe 1s
ATP levels Monroe 1s
ATP levels Monroe 1s
ATP levels Monroe 1s
ATP levels Monroe 1s
ATP levels Monroe 1s
ATP levels Monroe 1s
ATP levels Monroe 1s
Operation properties:
Shaking duration 1.0 s
Shaking speed Normal
Shaking diameter 0.10 mm
Shaking type Linear
Repeated operation Yes
Dispenser head control:
When measuring, keep injector head above well.
Dispense and measure simultaneously.
Ready

APPENDIX C - PLAN OF STUDY

Transfer Credit – Oklahoma State University

Semester	7000 Level	Credits
Spring 2008	ETM 5111 - Introduction to Strategy, Technology, and Integration	1
Spring 2008	IEM 5623 - Project Planning & Control Techniques	3
Summer 2008	ETM 5251 - Problem Solving & Decision Making	1
Summer 2008	ETM 5311 - Value Engineering	1
Fall 2008	IEM 5503 - Finance and Advanced Capital Investment Analysis	3
Spring 2009	ETM 5341 - Leadership Strategies	1
Spring 2009	ETM 5351 - Planning Technical Projects	1
Summer 2009	ETM 5381 - Design & Implementing Change in Technical Mgmt	1
		12

LSU Credit

Semester	4000 Level	Credits
Fall 2007	IE 4520 - Supply Chain Logistics	3
Spring 2011	Math 4999 - Independent Study	3
Spring 2011	BE 4989 - Tissue Engineering	3
		9

Semester	7000 Level	Credits
Spring 2011	BE 7500 - Seminar	1
Spring 2011	BE 8000 - Thesis	3
Summer 2011	BE 7909 - Independent Study	3
Summer 2011	BE 8000 - Thesis	3
		10

Total Hours	**31**
4000 Level	9
7000 Level (includes 5000 level at OSU)	22

At least half of all hours must be at or above the 7000 Level
Must include one advanced math class
Must include BE 7500 Seminar

APPENDIX D – LIST OF ABBREVIATIONS

ATP	adenosine 5'-triphosphate
DMNB	4,5-dimethoxy-2-nitrobenzyl
DMNB-NH2	4,5-dimethoxy-2-nitrobenzylamine
DMNPE	1-(4,5-dimethoxy-2-nitrophenyl)diazoethane
DMSO	dimethyl sulfoxide
DNA	deoxyribonucleic acid
dsRNA	double-stranded RNA
ESI-MS	electrospray ionization mass spectroscopy
HPLC	high performance liquid chromatography
MALDI-MS	matrix-assisted laser desorption/ionization mass spectroscopy
mG	5' methylated guanosine triphosphate
miRNA	microRNA
mRNA	messenger RNA
MS	mass spectroscopy
NA	nucleic acid
NB	2-nitrobenzyl
NB-NH_2	2-nitrobenzylamine
NPE	1-(2-nitrophenyl)ethyl
nt	Nucleotide
NTP	Nucleoside triphosphate
poly-A	poly-adenosine
PTGS	post transcriptional gene silencing
Rf	resolution factor
RISC	RNA-induced silencing complex
RLU	Relative luminescence unit
RNA	ribonucleic acid
RNAi	RNA interference
rNTP	ribonucleotide tri-phosphate
RP-HPLC	Reverse phase high performance liquid chromatography
shRNA	short hairpin RNA
siRNA	small interfering RNA
TEA	triethylammonium
TEAA	triethylammonium acetate
TPE	two-photon excitation

VITA

Amanda Yoesting Hendrix, daughter of Kent and Cindy Yoesting, was born in Tulsa, Oklahoma. She grew up in Houston, Texas and graduated from James E. Taylor High School, Katy, Texas. In 2005, she earned her Bachelor of Science in Mechanical Engineering and Honors Degree *Summa Cum Laude* from Oklahoma State University in Stillwater, Oklahoma. While at Oklahoma State, she was named Oklahoma State Regents Scholar, and as a College of Engineering, Architecture and Technology Scholar she traveled to Washington, D.C. and Japan on industry study travel awards. Afterward, she worked as a pipeline field engineer for ExxonMobil Pipeline Company in Houston and Baton Rouge, Louisiana. Amanda married her husband Jake Hendrix in the fall of 2009. In 2010, she started classes at Louisiana State University toward a career change to biological engineering. In fall 2010, she began teaching in the Biological & Agricultural Engineering department as the Teaching Associate, and began her Master of Science in Biological Engineering with research in the laboratory of Dr. W. Todd Monroe. Starting in August 2011, she began her PhD at Baylor College of Medicine in Houston, Texas, in the interdepartmental program of Translational Biology and Molecular Medicine. She was named the Howard Hughes Medical Institute Med-Into-Grad Scholar for her entering class of students.